Lattice Vibrations and the Accurate Determination of Structure Factors for the Elastic Scattering of X-rays and Neutrons

By B. T. M. Willis

Atomic Energy Research Establishment, Harwell, England

Two basic assumptions are usually made by crystallographers in the evaluation of X-ray or neutron structure factors. The first is the validity of the harmonic approximation in deriving the Debye–Waller factors which account for the effect of lattice vibrations in reducing the intensities of the Bragg reflexions. The second assumption is that the contribution to the measured intensity of thermal diffuse scattering (TDS), which rises to a peak at the reciprocal lattice point, can be ignored. Anharmonicity and TDS can each give rise to appreciable intensity effects, and so must be allowed for in accurate work. Anharmonicity can be taken into account by treating the crystal as a system of independent anharmonic oscillators, with each atom vibrating in a potential field whose symmetry conforms with the site symmetry of the atom. The effect of TDS can be calculated approximately using first-order (one-phonon) harmonic scattering theory, together with a knowledge of the elastic constants of the crystal. Calculations of both types of correction are considered in detail for a cubic crystal, and are applied to the analysis of X-ray diffraction measurements on KCl and of neutron measurements on BaF_2.

A. INTRODUCTION
1. General

In this article we shall discuss certain limitations in the conventional procedure of determining structure factors from the experimental measurement of Bragg intensities. The limitations are of two kinds, and both are concerned with the influence of lattice vibrations on the interpretation of the intensity measurements. The first relates to the use of the harmonic approximation in evaluating, by means of the Debye–Waller
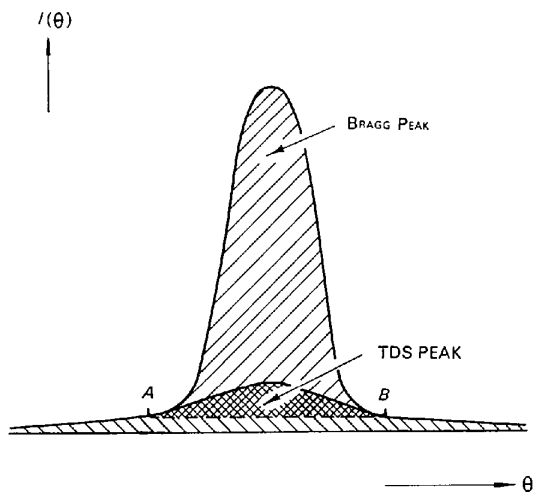

Fig. 1. Intensity scattered in the region of the Bragg peak. The total intensity from both Bragg scattering and thermal diffuse scattering is represented by the area above the straight line *AB*. The cross-hatched region denotes the intensity from thermal diffuse scattering alone (after Cooper, 1969).

theory*, the 'temperature factors' of the individual atoms in the unit cell. A crystal with harmonic interatomic forces would have no thermal expansion and many other properties not possessed by real crystals; it is not surprising, therefore, that the Debye–Waller theory fails to account completely for the effect of thermal motion in reducing the intensities of the Bragg reflexions. Lonsdale (1962) has commented that the Debye–Waller theory has '... never been extended quantitatively ... to temperatures near the melting point, where anharmonic vibrations become increasingly important.' Anharmonic effects are even present at 0°K, but we shall be concerned mainly with room temperature or above, as most of the available experimental measurements lie in this range. The second kind of limitation concerns the thermal diffuse scattering (TDS) which is distributed throughout reciprocal space and rises to a peak at the reciprocal lattice points (see Fig. 1). It is normally assumed that the integrated Bragg intensity, associated with the elastic scattering process only, is given by the area lying above the straight line *AB* joining the background on either side of the Bragg peak; this procedure ignores the inelastic contribution from TDS, which is represented by the cross-hatched region in Fig. 1 and can constitute an appreciable fraction of the total area.

---

* The extension of the Debye–Waller theory to the scattering of neutrons is due to Weinstock, Waller and others: the expression 'Debye–Waller theory' will be employed in discussing both X-rays and neutrons. We shall use 'Debye–Waller factor' to denote the reduction in intensity of an X-ray or neutron reflexion caused by thermal vibration, and 'temperature factor' as the corresponding quantity multiplying the atomic scattering factor (X-rays) or the nuclear scattering length (neutrons).

The Debye–Waller (harmonic) theory forms the starting point of our discussion. The theory, as applied to X-ray scattering (James, 1962; Cochran, 1963; Slater, 1967) and to neutron scattering (Cochran, 1963; Egelstaff, 1965), is fully described elsewhere. In the next section, we shall quote results from this theory, without proof; these results will be used later in discussing our two main issues, anharmonicity and TDS.

In Part B anharmonic effects are considered. § 3 describes the formal problem of extending the Debye–Waller theory to include cubic-anharmonic and quartic-anharmonic terms in the potential energy of the crystal: the solution of this problem is extremely difficult, and has been attempted only for crystals with the rocksalt structure and for certain monatomic cubic crystals. This difficulty arises because the displacement of a given atom is governed by the displacements of all the remaining atoms. A simpler theoretical approach, which gives essentially the same expressions for the temperature factors of these simple structures as the coupled-oscillator treatment, assumes that the atomic displacements are independent of one another. The temperature factors for such an Einstein solid are derived in § 4 for atoms occupying sites with different types of cubic point symmetry. In § 5, the structure factors are calculated for a few standard cubic structures, using the results of the previous section in combination with the generalized structure-factor formalism proposed by Dawson (1967a). The very limited experimental data on anharmonicity is discussed in § 6, where it is shown that the Einstein theory provides a satisfactory interpretation of the observed X-ray intensities from KCl and neutron intensities from BaF_2.

The effect of thermal diffuse scattering on the measured intensities is treated in Part C. § 7 deals with the theory of first-order (one-phonon) TDS contributions to the peak observed with X-rays, and § 8 with the corresponding theory for neutrons. Unlike the zero-order intensity, the TDS peak depends on correlation between the motion of different atoms, and so it is essential to adopt a coupled-oscillator model of the crystal. However, the theory of TDS based on the harmonic approximation, using the relevant cross-section formulae quoted in Part A, will be adequate for our purpose. In § 9, the theory is applied to the correction of intensities recorded on KCl (X-rays) and BaF_2 (neutrons).

2. Scattering formulae based on the harmonic approximation

2·1. List of symbols

The influence of lattice vibrations on the scattering of X-rays by single crystals has been treated by many authors, some of them using their own particular brand of notation. We shall adopt the notation of Cochran (1963), which converts readily from X-ray scattering to neutron scattering: a list of the symbols is given in Table 1. Note that the unit cells of the direct lattice,

defined by a_1, a_2, a_3, and of the reciprocal lattice, defined by b_1, b_2, b_3, are related by

$$a_i \cdot b_i = 2\pi \qquad (2\cdot1)$$
$$(i = 1, 2, 3).$$

The volume of the reciprocal unit cell is

$$v_z = 8\pi^3/v,$$

where v is the volume of the direct unit cell; the radius of the Ewald sphere is $2\pi/\lambda$. The advantage of using (2·1), which differs from the usual definition of the reciprocal lattice used in crystallography, is that many of the formulae given later are simplified by the omission of 2π. Our reciprocal lattice vector B is related to the reciprocal lattice vector s used by other authors (e.g. Cruickshank, 1956) by

$$B \equiv 2\pi s.$$

For Bragg scattering, the scattering vector Q is equivalent to B so that Q and B are interchangeable in the formulae for the Debye–Waller factor quoted in Parts A and B.

Table 1. Definition of symbols

$h_1 h_2 h_3$	Miller indices
m_κ	mass of the κth atom in (direct)unit cell
n	number of atoms in unit cell
m	mass of unit cell $[m = \sum_\kappa m_\kappa]$
l	label identifying lth unit cell
N	number of unit cells in crystal
m_n	mass of neutron
λ	wavelength of X-rays or neutrons
k_0	wave vector of incident X-rays or neutrons $[k_0 = 2\pi/\lambda]$
k	wave vector of scattered X-rays or neutrons $[k = 2\pi/\lambda$ for X-ray scattering]
2θ	scattering angle, or angle between k_0 and k
θ_B	Bragg angle
Q	scattering vector ($\equiv k - k_0$) $[Q = 4\pi \sin \theta/\lambda]$
B	reciprocal lattice vector, or diffraction vector $[B = 4\pi \sin \theta_B/\lambda]$
f_κ	X-ray atomic scattering factor of κth atom (at rest)
b_κ	coherent nuclear scattering length of κth atom
a_i	unit cell vectors
b_i	reciprocal cell vectors $[a_i \cdot b_j = 2\pi\delta_{ij}]$
v	volume of unit cell
v_z	volume of reciprocal cell
q	wave vector of elastic wave. For each q, there are $3n$ normal modes of vibration
$e_j(q)$	polarization vector of mode (j, q) $[1 \le j \le 3n]$
$\omega_j(q)$	circular frequency of mode (j, q)
$E_j(q)$	energy of mode (j, q)
$\alpha_j(q)$	angle between Q and polarization direction of mode (j, q)
$r(l\kappa)$	radius vector from a fixed origin in the crystal to equilibrium position of κth atom in lth cell
$u(l\kappa)$	displacement of atom (l, κ) from its equilibrium position
$u_1 u_2 u_3$	cartesian components of u
$2W(Q)$	exponent of Debye–Waller factor, exp $[-2W(Q)]$
$W_\kappa(Q)$	exponent of temperature factor, exp $[-W_\kappa(Q)]$, of κth atom
$T_\kappa(Q)$	temperature factor of κth atom $[T_\kappa(Q) = e^{-W_\kappa(Q)}]$
k_B	Boltzmann's constant
T	temperature in $^\circ$K
$\hbar$	Planck's constant divided by 2π
γ_G	Grüneisen constant
χ	volume expansion coefficient

2·2. X-ray scattering

From the kinematic theory of diffraction, the amplitude of scattering of X-rays from a crystal is proportional to

$$Y(\mathbf{Q}) = \sum_{l\kappa} f_\kappa \exp\left[i\mathbf{Q} \cdot (\mathbf{r}(l\kappa) + \mathbf{u}(l\kappa))\right]$$

where the summation is over the n atoms of the unit cell $(1 \le \kappa \le n)$ and over the N cells of the crystal $(1 \le l \le N)$.

The differential scattering cross-section, $d\sigma/d\Omega$, giving the intensity of scattering into unit solid angle for unit incident intensity, is YY^*:

$$\frac{d\sigma}{d\Omega} = \sum_{l\kappa} \sum_{l'\kappa'} f_\kappa f_{\kappa'} \exp[i\mathbf{Q} \cdot (\mathbf{r}(l\kappa)$$
$$-\mathbf{r}(l'\kappa'))]\langle \exp[i\mathbf{Q} \cdot (\mathbf{u}(l\kappa) - \mathbf{u}(l'\kappa'))]\rangle . \quad (2\cdot2)$$

The displacements $\mathbf{u}(l\kappa)$ are time-dependent, and the angle brackets $\langle\,\rangle$ indicate the average value over a period of time which is long compared with the period of vibration of an individual atom.

The various scattering processes contributing to $\dfrac{d\sigma}{d\Omega}$ can be subdivided into the elastic (zero-order) process and inelastic processes, involving exchange of energy with the quanta of lattice vibrational energy, or phonons, of the crystal. Thus

$$\frac{d\sigma}{d\Omega} = \left(\frac{d\sigma}{d\Omega}\right)_0 + \left(\frac{d\sigma}{d\Omega}\right)_1 + \left(\frac{d\sigma}{d\Omega}\right)_2 + \dots \quad (2\cdot3)$$

where the successive terms on the right-hand side represent the cross-sections for zero-order (zero-phonon), first order (one-phonon), second order (two-phonon).. scattering.

To develop the expressions $(2\cdot2)$ and $(2\cdot3)$ further we expand the potential energy V of the crystal as a Taylor power series in the cartesian components $u_{x_1}(l\kappa)$, $u_{x_2}(l\kappa)$, $u_{x_3}(l\kappa)$ of the thermal displacements $\mathbf{u}(l\kappa)$ of all the atoms:

$$V = V_0 + \sum_{xl\kappa} u_x(l\kappa)\left[\frac{\partial V}{\partial x(l\kappa)}\right]_0$$
$$+ \sum_{xl\kappa}\sum_{x'l'\kappa'} u_x(l\kappa)u_{x'}(l'\kappa')\left[\frac{\partial^2 V}{\partial x(l\kappa)\partial x'(l'\kappa')}\right]_0$$
$$+ \text{higher-order terms} \dots \quad (2\cdot4)$$

The zero subscripts in $(2\cdot4)$ mean that the derivatives are evaluated at the equilibrium positions $\mathbf{r}(l\kappa)$ of the atoms, so that the linear term

$$\sum_{xl\kappa} u_x(l\kappa)\left[\frac{\partial V}{\partial x(l\kappa)}\right]_0$$

vanishes. In the 'harmonic approximation', all the higher-order terms after the quadratic term in $(2\cdot4)$ are ignored.

Using this approximation, the cross-section for Bragg scattering reduces to

$$\left(\frac{d\sigma}{d\Omega}\right)_0 = Nv_z \sum_{\mathbf{B}} |F(\mathbf{B})|^2 \delta(\mathbf{Q} - \mathbf{B}) , \quad (2\cdot5)$$

where

$$F(\mathbf{Q}) = \sum_{\kappa=1}^{n} f_\kappa(\mathbf{Q}) \exp[-W_\kappa(\mathbf{Q})] \exp[i\mathbf{Q} \cdot \mathbf{r}(\kappa)] . \quad (2\cdot6)$$

The delta function $\delta(\mathbf{Q} - \mathbf{B})$ represents the condition that scattering cannot take place unless $\mathbf{Q} = \mathbf{B}$, or $2\sin\theta/\lambda = 1/d$: it is defined by the equations

$$\left.\begin{array}{l} \delta(\mathbf{Q} - \mathbf{B}) = 0 \text{ for } \mathbf{Q} \neq \mathbf{B} \\[2mm] \int \delta(\mathbf{Q} - \mathbf{B})dv_z = 1 , \end{array}\right\}$$

where the integration is over the Brillouin zone associated with $\mathbf{B}$. Equation $(2\cdot6)$ is the structure-factor expression for elastic scattering. $\mathbf{r}(\kappa)$ is the radius vector from the origin of the unit cell to the equilibrium position of the κth atom, and $\exp[-W_\kappa(\mathbf{Q})]$ is the temperature factor accounting for the influence of the thermal motion of the κth atom.

The exponent of the temperature factor is given by:

$$\left.\begin{array}{l} W_\kappa = \frac{1}{2}\langle[\mathbf{Q} \cdot \mathbf{u}(l\kappa)]^2\rangle \\[2mm] = \frac{1}{2}Q^2\langle u^2\rangle_Q , \end{array}\right\} \quad (2\cdot7)$$

where $\langle u^2\rangle_Q$ is the mean square amplitude of vibration along $\mathbf{Q}$. $\langle u^2\rangle_Q$ can be expressed as a symmetrical tensor; with a maximum number of six independent components. For a cubic crystal with atoms occupying sites of cubic symmetry, there is only one independent component as $\langle u^2\rangle_Q$ is isotropic. In this case, W_κ can be written

$$W_\kappa = B_\kappa \sin^2\theta/\lambda^2 \quad (2\cdot8a)$$

where the isotropic B factor of the κth atom is

$$B_\kappa = 8\pi^2\langle[u(l\kappa)]^2\rangle . \quad (2\cdot8b)$$

The contribution of an individual mode of vibration $(j\mathbf{q})$ of a cubic crystal to the mean square displacement $\langle[u(l\kappa)]^2\rangle$ in any direction is proportional to

$$\frac{E_j(\mathbf{q})}{\omega_j^2(\mathbf{q})} . \quad (2\cdot9)$$

At high temperatures, in the region of equipartition, . the mode energy $E_j(\mathbf{q}) = k_B T$. Thus, provided the frequencies $\omega_j(\mathbf{q})$ are temperature-independent, W_κ is proportional to the absolute temperature.

The scattering theory based on the harmonic approximation leads, therefore, to the important results:

(i) W_κ contains terms which are quadratic in $\mathbf{Q}$ (equation $2\cdot7$), but does not contain any higher-order terms;

(ii) W_κ is proportional to T at high temperatures .

In the modification of the harmonic theory which allows for the influence of lattice expansion on the frequencies $\omega_j(\mathbf{q})$ ('quasi-harmonic theory': see section 4·3), W_κ is quadratic in $\mathbf{Q}$ but contains terms in both T and T^2. We shall see in Part B that anharmonicity leads to a more complex dependence of W_κ on both $\mathbf{Q}$ and T.

The cross-section for first-order scattering, $(d\sigma/d\Omega)$ in equation (2·3), involves the $3nN$ modes of vibration. The cross-section for the $3n$ modes with the same wave vector $\mathbf{q}$ is:

$$\left(\frac{d\sigma(\mathbf{q})}{d\Omega}\right)_1 = \frac{NQ^2}{m} \sum_{j=1}^{3n} \frac{E_j(\mathbf{q})}{\omega_j^2(\mathbf{q})} |G_j(\mathbf{Q})|^2 \quad (2\cdot10)$$

where $\mathbf{Q}$ and $\mathbf{q}$ are related by the condition

$$\mathbf{Q}+\mathbf{q}=\mathbf{B}$$

and $G_j(\mathbf{Q})$ is the so-called 'structure factor for first-order scattering'. We shall apply formula (2·10) in Part C to the scattering from acoustic modes of small wave vector: for these elastic waves, we can write

$$G_j(\mathbf{Q})=F(\mathbf{Q}) \cos \alpha_j(\mathbf{q}) ,$$

so that (2·10) becomes

$$\left(\frac{d\sigma(\mathbf{q})}{d\Omega}\right)_1 = \frac{NQ^2}{m} \sum_{j=1}^{3} \frac{E_j(\mathbf{q})}{\omega_j^2(\mathbf{q})} |F(\mathbf{Q})|^2 \cos^2\alpha_j(\mathbf{q}) \quad (2\cdot10a)$$

where the summation is restricted to the three acoustic modes of wave vector $\mathbf{q}$.

We do not need the formulae for second-order or higher-order scattering $\left[i.e. \left(\dfrac{d\sigma}{d\Omega}\right)_2, \left(\dfrac{d\sigma}{d\Omega}\right)_3 \text{ in equa-}\right.$ tion(2·3) $\Big]$, but in Fig.2 we illustrate the geometrical conditions governing the zero-order, first-order, second-order scattering processes. These diagrams are helpful in visualizing the nature of the various scattering processes.

2·3. Neutron scattering

For an element containing a mixture of different isotopes, or for a single isotope with non-zero nuclear spin, the scattering length for slow neutrons varies from one atom to another, and the total scattering is partly coherent and partly incoherent. The coherent scattering gives rise to interference effects, and is computed by replacing the scattering length of each atom by the average scattering length of the corresponding element. The incoherent scattering merely increases the background scattering level in a diffraction experiment, and will not concern us further.

The expression giving the differential scattering cross-section for the coherent elastic scattering of neutrons is the same as for X-rays, equations (2·5) and

(2·6), with b_κ replacing f_κ. Thus the structure factor for the Bragg scattering of neutrons is

$$F(\mathbf{Q})= \sum_\kappa b_\kappa \exp\left[- W_\kappa(\mathbf{Q})\right] \exp\left[i\mathbf{Q}\cdot\mathbf{r}(\kappa)\right]. \quad (2\cdot11)$$

Note that b_κ is independent of $\mathbf{Q}$ and is usually independent of the wavelength of the neutrons too: this is in contrast with the X-ray scattering factor f_κ, which varies with θ (form-factor dependence) and λ (anomalous dispersion).
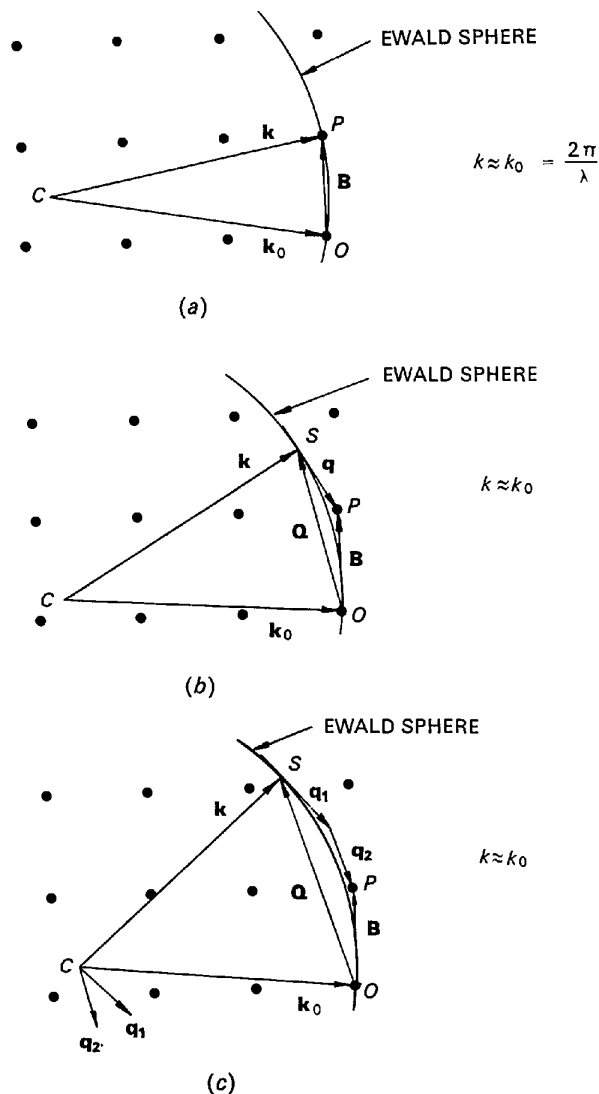

Fig. 2. Reciprocal lattice diagrams representing: (a) zero-order (Bragg) scattering of X-rays, (b) first-order scattering of X-rays, (c) second-order scattering of X-rays. O is the origin of reciprocal space, P is the reciprocal lattice point, C is the centre of the Ewald sphere, and $\overrightarrow{CS}$ (=$\mathbf{k}$) in (b) and (c) is the wave vector of the scattered X-rays. The two wave vectors $\mathbf{q}_1$ and $\mathbf{q}_2$ in (c) add vectorially to equal $\overrightarrow{SP}$.

The inelastic coherent first-order scattering is governed by the momentum conservation rule

$$Q+q=B \qquad (2\cdot12a)$$

and by the energy conservation rule

$$\frac{\hbar^2}{2m_n}(k^2-k_0^2)=\pm\hbar\omega_j(q) . \qquad (2\cdot12b)$$

The minus sign in $(2\cdot12b)$ corresponds to the phonon absorption process in which the neutron gains energy, and the positive sign to the phonon emission process in which the neutron loses energy. The same conservation rules apply to first-order X-ray scattering, but, as the phonon energy $\hbar\omega_j(q)$ is negligible compared with the energy of the X-ray phonon, $(2\cdot12)$ reduces

to $k=k_0$ (see Fig.2). The energy of slow neutrons is comparable with phonon energies, and so the scattering surface, giving the locus of points in reciprocal space satisfying the scattering conditions $(2\cdot12)$, is more complicated than for X-rays (see Fig.3). The scattering surface is different for phonon absorption and phonon emission, and each branch j of the phonon dispersion curves can have its own distinct pair of scattering surfaces. For this reason, the evaluation of the TDS correction for neutrons, discussed in Part C, is less straightforward than for X-rays.

The cross-section for coherent first-order scattering involving modes with wave vector q is

$$\left(\frac{d\sigma(q)}{d\Omega}\right)_1=\frac{NQ^2}{2m}\frac{k}{k_0}$$
$$\times\sum_{j=1}^{3n}\frac{E_j(q)\pm\frac{1}{2}\hbar\omega_j(q)}{|J_j|\omega_j^2(q)}|G_j(Q)|^2 \qquad (2\cdot13)$$

which is to be compared with the corresponding X-ray formula $(2\cdot10)$. The Jacobian J_j can be expressed in terms of the neutron velocity V_n and the group velocity $V_j(q)$ of the mode (jq):

$$|J_j|=1\pm\frac{V_n . V_j(q)}{V_n^2} . \qquad (2\cdot14)$$

The cross-section for phonon emission is obtained by choosing the positive sign in $(2\cdot13)$ and $(2\cdot14)$, and the cross-section for phonon absorption by choosing the negative sign.

In Part B we shall consider the modification of the zero-order scattering formulae to account for anharmonicity, and in Part C we shall use the first-order scattering formulae to evaluate the TDS correction. We shall not consider the effect of anharmonicity on the first-order cross-section: readers interested in this subject are referred to Kashiwase (1965) (X-rays) and to Thompson (1963) (neutrons).

B. EFFECT OF ANHARMONICITY ON THE MEASURED INTENSITIES
3. Theory for coupled anharmonic oscillators

To obtain a general expression for the Bragg intensity, which includes anharmonic contributions to the Debye–Waller factor, we return to equation $(2\cdot2)$. In the classical or 'high temperature' limit, the time average in this equation can be evaluated as an ensemble average using the expression

$$\langle\exp[i\mathbf{Q} . (\mathbf{u}(lk)-\mathbf{u}(l'k'))]\rangle$$

$$=\left(\int\!\!\int\!\!\int\ldots\int\exp(-V/k_BT)\exp[i\mathbf{Q} . (\mathbf{u}(lk)\right.$$

$$\left.-\mathbf{u}(l'k'))]dx_1dx_2dx_3\ldots dx_{3nN}\right)\Big/$$

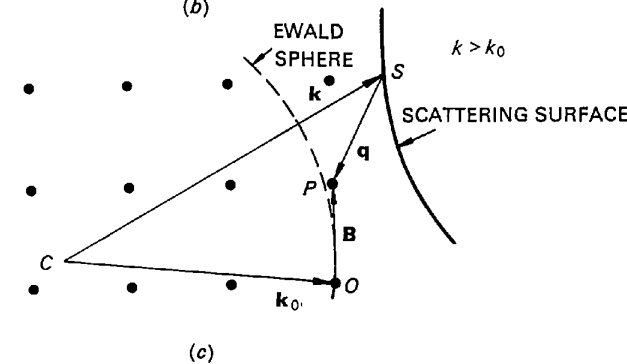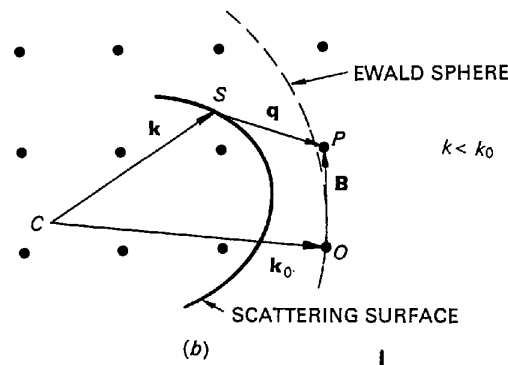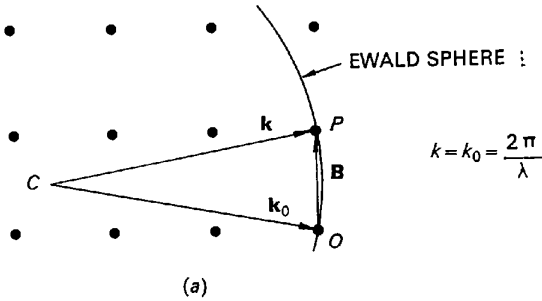$$\left(\int\!\!\int\!\!\int\ldots\int\exp(-V/k_BT)dx_1dx_2dx_3\ldots dx_{3nN}\right) \qquad (3\cdot1)$$

Fig.3. Reciprocal lattice diagrams representing: (a) zero-order (Bragg) scattering of neutrons, (b) first-order scattering of neutrons with loss of neutron energy (phonon emission), (c) first-order scattering of neutrons with gain of neutron energy (phonon absorption). The scattering surfaces in (b) and (c) are shown schematically only: their exact shapes are determined by the conservation rules, equations (2.12).

where V is the potential energy of the total system of coupled oscillators, and the integration is carried out over the $3nN$ cartesian coordinates $dx_1 dx_2 dx_3 \ldots$ of the nN atoms in the crystal. The Debye–Waller factor is related to the cross-section for Bragg scattering, $\left(\dfrac{d\sigma}{d\Omega}\right)_0$, and is given by those terms in (3·1) which are independent of both $l\kappa$ and $l'\kappa'$: the remaining terms are related to the cross-sections for first-order, second-order ... thermal diffuse scattering, $\left(\dfrac{d\sigma}{d\Omega}\right)_1$, $\left(\dfrac{d\sigma}{d\Omega}\right)_2$ ... Thus the effect of thermal motion on the Bragg intensity is equivalent to multiplying the scattering amplitude of each atom $l\kappa$ by the temperature factor

$$T_\kappa(\mathbf{Q}) = \langle \exp[i\mathbf{Q}.\mathbf{u}(l\kappa)]\rangle \qquad (3·2)$$

where $\mathbf{u}(l\kappa)$ is the displacement of the κth atom in the lth cell.

Anharmonicity is taken into account in equation (3·1) by extending the expression (2·4) for the potential energy to include the cubic-anharmonic term

$$\sum_{x l \kappa}\sum_{x' l' \kappa'}\sum_{x'' l'' \kappa''} u_x(l\kappa)u_{x'}(l'\kappa')u_{x''}(l''\kappa'')$$

$$\times [\partial^3 V/\partial x(l\kappa)\partial x'(l'\kappa')\partial x''(l''\kappa'')]_0$$

and the quartic-anharmonic term

$$\sum_{x l \kappa}\sum_{x' l' \kappa'}\sum_{x'' l'' \kappa''}\sum_{x''' l''' \kappa'''} u_x(l\kappa)u_{x'}(l'\kappa')u_{x''}(l''\kappa'')u_{x'''}(l'''\kappa''')$$

$$\times [\partial^4 V/\partial x(l\kappa)\partial x'(l'\kappa')\partial x''(l''\kappa'')\partial x'''(l'''\kappa''')]_0 .$$

The calculation of the cubic-anharmonic and quartic-anharmonic contributions to the Debye–Waller factor from equation (3·1) has been attempted by a number of authors, including Krivoglaz & Tekhonova (1961), Hahn & Ludwig (1961), Maradudin & Flinn (1963) and Kashiwase (1965). Kashiwase's analysis was extended to low temperatures using quantum statistics, but in this paper we shall discuss only the classical high-temperature range, where anharmonic effects are expected to be largest. The most detailed analysis is that of Maradudin & Flinn, who considered a monatomic crystal with atoms arrayed at the points of a cubic Bravais lattice: their calculations are extremely lengthy, but the main results can be reproduced readily by using an Einstein model of the crystal (see section 4·4 below). By treating the crystal as an Einstein solid, whereby each atom vibrates in a potential field which is not affected by the motion of the neighbouring atoms, the evaluation of (3·1) is much simplified, and the extension of the anharmonic analysis to any type of crystal structure is then possible. It is well-known (e.g. James, 1962, page 25) that the harmonic theories based on coupled oscillations and on independent oscillations give equivalent results for the influence of temperature on the Bragg intensities.

4. Theory for independent anharmonic oscillators

The temperature factor $T_\kappa(\mathbf{Q}) \equiv \exp[-W_\kappa(\mathbf{Q})]$ is given by the average $\langle \exp(i\mathbf{Q}.\mathbf{u}_\kappa)\rangle$, where $\mathbf{u}_\kappa$ is the thermal displacement of atom κ. In the harmonic approximation, the average obeys a Gaussian distribution

$$W_\kappa = \tfrac{1}{2}\langle(\mathbf{Q}.\mathbf{u}_\kappa)^2\rangle$$

but anharmonicity introduces additional terms in W_κ which are of higher order in Q than quadratic.

For an Einstein solid, we can determine the quantity $\langle \exp(i\mathbf{Q}.\mathbf{u}_\kappa)\rangle$ by weighting each possible value of $\exp(i\mathbf{Q}.\mathbf{u}_\kappa)$ by its thermodynamic probability, using the equation [cf. equation (3·1)]:

$$\langle \exp(i\mathbf{Q}.\mathbf{u}_\kappa)\rangle$$

$$= \left(\iiint_{-\infty}^{\infty} \exp[-V_\kappa/k_BT]\exp(i\mathbf{Q}.\mathbf{u}_\kappa)du_1 du_2 du_3\right) \Big/$$

$$\left(\iiint_{-\infty}^{\infty} \exp[-V_\kappa/k_BT]du_1 du_2 du_3\right) . \qquad (4·1)$$

u_1, u_2, u_3 are the cartesian coordinates of the displacement $\mathbf{u}_\kappa$, and V_κ is the potential energy of the κth atom, vibrating as an anharmonic oscillator in the average force field of its neighbours. If V_κ is expanded as a power series in the coordinates u_1, u_2, u_3, referred to an origin at the equilibrium position of the atom, the integrals in the expression for the temperature factor reduce to standard forms. We shall illustrate this procedure by considering atoms with different types of cubic coordination in a cubic crystal.

4·1. *Potential of atom in cubic crystalline field*

In the harmonic approximation, the potential expansion terminates at the quadratic term and is of the form

$$V_\kappa = V_0 + \tfrac{1}{2}\alpha_\kappa(u_1^2 + u_2^2 + u_3^2) \qquad (4·2)$$

where the parameter α_κ is related to the mean-square displacement $\overline{u_\kappa^2}$, in any direction by

$$\alpha_\kappa = \frac{k_BT}{\overline{u_\kappa^2}} . \qquad (4·3)$$

Anharmonic modifications to V_κ are represented by third-order and higher-order terms added to the right-hand side of (4·2). These anharmonic terms are either isotropic (i.e. dependent on the magnitude only of $\mathbf{u}_\kappa$) or anisotropic.

Isotropic terms which can be added to (4·2) are of the form

$$\gamma_\kappa(u_1^2 + u_2^2 + u_3^2)^2 , \quad \varepsilon_\kappa(u_1^2 + u_2^2 + u_3^2)^3 , \qquad (4·4)$$

and are even-order in the powers of u_1, u_2, u_3. In general, there is a softening of the vibration at large amplitudes, so that the signs of the potential parameters $\gamma_\kappa, \varepsilon_\kappa \ldots$ are likely to be negative.

Anisotropic terms represent the influence of the local crystalline field in producing an angular dependence of the potential $V(u_1u_2u_3)$. They are written conveniently in such a way that their average value over the surface of the sphere of radius $r(r^2 = u_1^2 + u_2^2 + u_3^2)$ is nothing. The third-order anisotropic term appropriate to $\bar{4}3m$ point symmetry (e.g. diamond structure) is

$$\beta_\kappa u_1 u_2 u_3 . \qquad (4\cdot5)$$

This gives rise to four tetrahedral lobes along $\langle 111 \rangle$. We would expect the potential to increase along nearest-neighbour directions, so that β_κ is positive if the coordinate axes are chosen so that the atom κ has
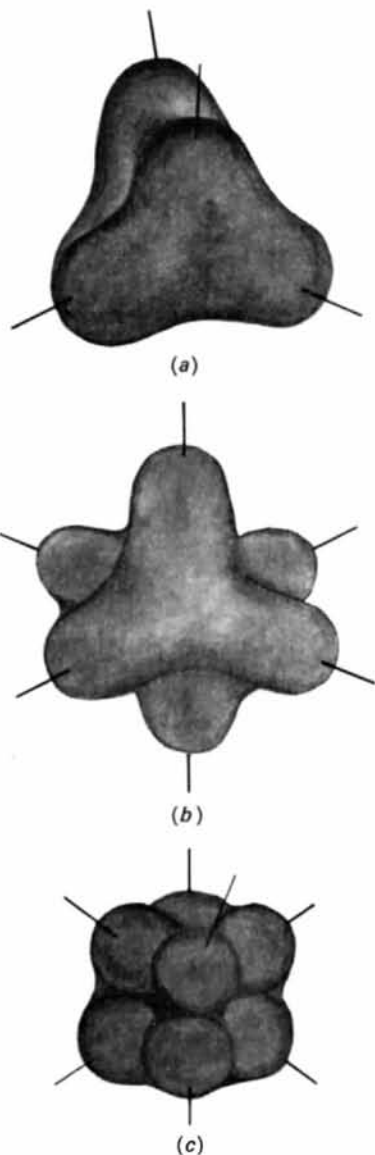

(a)

(b)

(c)

Fig. 4. Modification of isotropic potential function by: (a) third-order term $\beta u_1 u_2 u_3$, giving four tetrahedral lobes along $\langle 111 \rangle$; (b) fourth-order term with δ positive, giving six lobes along $\langle 100 \rangle$; (c) fourth-order term with δ negative, giving eight lobes along $\langle 111 \rangle$.

a nearest neighbour along [111] and β_κ is negative if the nearest neighbour is along [$\bar{1}\bar{1}\bar{1}$].

For an atom occupying a site with a centre of inversion, the odd-order terms in the expansion of V vanish and the first anisotropic term is fourth order, of the form

$$\delta_\kappa(u_1^4 + u_2^4 + u_3^4 - \tfrac{3}{5}r^4) . \qquad (4\cdot6)$$

For δ_κ positive, there are six lobes pointing along the $\langle 100 \rangle$ directions: this is appropriate, therefore, to atoms with octohedral coordination, as in the rocksalt structure. For δ_κ negative, there are eight lobes pointing along $\langle 111 \rangle$, and this would apply to the caesium chloride structure, with cubic (8-fold) coordination.

In the face-centred cubic structure, the atoms occupy sites of $m3m$ symmetry and are coordinated to twelve nearest neighbours along the $\langle 110 \rangle$ directions. To obtain a potential with twelve lobes along $\langle 110 \rangle$ it would be necessary to develop the expansion of $V_\kappa(u_1u_2u_3)$ to sixth order. A suitable anisotropic term for this case is

$$\mu_\kappa[u_1^6 + u_2^6 + u_3^6 + \tfrac{15}{4}(u_1^2u_2^4 + u_2^2u_3^4 + u_3^2u_1^4 \\ + u_1^4u_2^2 + u_2^4u_3^2 + u_3^4u_1^2) - \tfrac{15}{14}r^6] \quad (4\cdot7)$$

where μ_κ is positive.

All the functions (4·2) to (4·7) possess local cubic symmetry, and the anisotropic terms (4·5), (4·6) and (4·7) are related to the first few α-type and β-type 'Kubic Harmonics' of von der Lage & Bethe (1947). The properties of some of these functions are illustrated schematically in Fig. 4. It is straightforward to write down corresponding functions for sites of noncubic symmetry, but the number of independent parameters increases as the symmetry falls.

By terminating the potential expansion at the fourth-order (quartic) terms, a suitable general expression for the potential of the κth atom in a cubic crystalline field is

$$V_\kappa(u_1u_2u_3) = V_0 + \tfrac{1}{2}\alpha_\kappa r^2 + \beta_\kappa u_1 u_2 u_3 \\ + \gamma_\kappa r^4 + \delta_\kappa(u_1^4 + u_2^4 + u_3^4 - \tfrac{3}{5}r^4) , \quad (4\cdot8)$$

where $r^2 = u_1^2 + u_2^2 + u_3^2$. $\beta_\kappa = 0$ when the atomic site coincides with a centre of symmetry. This expression will be used for all cases considered below.

4·2. *Temperature factor of atom in cubic crystalline field*

If the displacement $\mathbf{u}_\kappa$ is such that the anharmonic terms in the potential (4·8) are small compared with $k_B T$, we can write

$$\exp\left[-V_\kappa(u_1u_2u_3)/k_B T\right] = \exp\left[-V_0/k_B T\right]$$
$$\times \exp\left[-\tfrac{1}{2}\alpha_\kappa(u_1^2 + u_2^2 + u_3^2)/k_B T\right]$$
$$\times \left\{ 1 - \frac{\beta_\kappa}{k_B T}\, u_1 u_2 u_3 - \frac{\gamma_\kappa}{k_B T}\,(u_1^2 + u_2^2 + u_3^2)^2 \right.$$
$$\left. - \frac{\delta_\kappa}{k_B T}\,(u_1^4 + u_2^4 + u_3^4 - \tfrac{3}{5}r^4) \right\} .$$

Inserting this into the expression (4·1) for the temperature factor, and replacing $\mathbf{Q} \cdot \mathbf{u}_\kappa$ by $\dfrac{2\pi}{a_0}$ $(h_1u_1 + h_2u_2 + h_3u_3)$ where a_0 is the cubic lattice parameter, we obtain

$$\exp[-W_\kappa(\mathbf{Q})] = M/N$$

where

$$M = \iiint_{-\infty}^{\infty} \exp[-\tfrac{1}{2}\alpha_\kappa(u_1^2 + u_2^2 + u_3^2)/k_BT]$$

$$\times \exp\left[\frac{2\pi i}{a_0}(h_1u_1 + h_2u_2 + h_3u_3)\right] du_1 du_2 du_3$$

$$-\frac{\beta_\kappa}{k_BT} \iiint_{-\infty}^{\infty} u_1 u_2 u_3 \exp[-\tfrac{1}{2}\alpha_\kappa(u_1^2 + u_2^2 + u_3^2)/k_BT]$$

$$\times \exp\left[\frac{2\pi i}{a_0}(h_1u_1 + h_2u_2 + h_3u_3)\right] du_1 du_2 du_3$$

$$-\frac{(\gamma_\kappa - \tfrac{2}{5}\delta_\kappa)}{k_BT} \iiint_{-\infty}^{\infty} (u_1^4 + u_2^4 + u_3^4)$$

$$\times \exp[-\tfrac{1}{2}\alpha_\kappa(u_1^2 + u_2^2 + u_3^2)/k_BT]$$

$$\times \exp\left[\frac{2\pi i}{a_0}(h_1u_1 + h_2u_2 + h_3u_3)\right] du_1 du_2 du_3$$

$$-\frac{2(\gamma_\kappa + \tfrac{3}{5}\delta_\kappa)}{k_BT} \iiint_{-\infty}^{\infty} (u_1^2 u_2^2 + u_2^2 u_3^2 + u_3^2 u_1^2)$$

$$\times \exp[-\tfrac{1}{2}\alpha_\kappa(u_1^2 + u_2^2 + u_3^2)/k_BT]$$

$$\times \exp\left[\frac{2\pi i}{a_0}(h_1u_1 + h_2u_2 + h_3u_3)\right] du_1 du_2 du_3 \quad (4\cdot9)$$

and

$$N = \iiint_{-\infty}^{\infty} \exp[-\tfrac{1}{2}\alpha_\kappa(u_1^2 + u_2^2 + u_3^2)/k_BT] du_1 du_2 du_3$$

$$-\frac{\beta_\kappa}{k_BT} \iiint_{-\infty}^{\infty} u_1 u_2 u_3 \exp[-\tfrac{1}{2}\alpha_\kappa$$

$$\times (u_1^2 + u_2^2 + u_3^2)/k_BT] du_1 du_2 du_3$$

$$-\frac{(\gamma_\kappa + \tfrac{2}{5}\delta_\kappa)}{k_BT} \iiint_{-\infty}^{\infty} (u_1^4 + u_2^4 + u_3^4)$$

$$\times \exp[-\tfrac{1}{2}\alpha_\kappa(u_1^2 + u_2^2 + u_3^2)/k_BT] du_1 du_2 du_3$$

$$-\frac{2(\gamma_\kappa - \tfrac{3}{5}\delta_\kappa)}{k_BT} \iiint_{-\infty}^{\infty} (u_1^2 u_2^2 + u_2^2 u_3^2 + u_3^2 u_1^2)$$

$$\times \exp[-\tfrac{1}{2}\alpha_\kappa(u_1^2 + u_2^2 + u_3^2)/k_BT] du_1 du_2 du_3. \quad (4\cdot10)$$

All the integrals in (4·9) and (4·10) can be evaluated using the standard relations:

$$\iiint_{-\infty}^{\infty} \exp[-A(u_1^2 + u_2^2 + u_3^2)]$$

$$\times \exp[2iB(h_1u_1 + h_2u_2 + h_3u_3)] du_1 du_2 du_3 = P,$$

$$\iiint_{-\infty}^{\infty} u_1 u_2 u_3 \exp[-A(u_1^2 + u_2^2 + u_3^2)]$$

$$\times \exp[2iB(h_1u_1 + h_2u_2 + h_3u_3)] du_1 du_2 du_3$$

$$= -\frac{iB^3}{A^3} h_1 h_2 h_3 P,$$

$$\iiint_{-\infty}^{\infty} (u_1^4 + u^4 + u_3^4) \exp[-A(u_1^2 + u_2^2 + u_3^2)]$$

$$\times \exp[2iB(h_1u_1 + h_2u_2 + h_3u_3)] du_1 du_2 du_3$$

$$= \left[\frac{9}{4A^2} - \frac{3B^2}{A^3}(h_1^2 + h_2^2 + h_3^2) + \frac{B^4}{A^4}(h_1^4 + h_2^4 + h_3^4)\right] P,$$

$$\iiint_{-\infty}^{\infty} (u_1^2 u_2^2 + u_2^2 u_3^2 + u_3^2 u_1^2) \exp[-A(u_1^2 + u_2^2 + u_3^2)]$$

$$\times \exp[2iB(h_1u_1 + h_2u_2 + h_3u_3)] du_1 du_2 du_3$$

$$= \left[\frac{3}{4A^2} - \frac{B^2}{A^3}(h_1^2 + h_2^2 + h_3^2)\right.$$

$$\left. + \frac{B^4}{A^4}(h_1^2 h_2^2 + h_2^2 h_3^2 + h_3^2 h_1^2)\right] P,$$

where

$$P = \left(\frac{\pi}{A}\right)^{3/2} \exp\left[-\left(\frac{B^2}{A}\right)(h_1^2 + h_2^2 + h_3^2)\right].$$

The final expression for the temperature factor works out as:

$$\exp[-W_\kappa(\mathbf{Q})] = N_\kappa \exp\left[-\frac{Q^2 k_BT}{2\alpha_\kappa}\right]$$

$$\times \left\{1 - 15k_BT\left(\frac{\gamma_\kappa}{\alpha_\kappa^2}\right)\right.$$

$$+ 10(k_BT)^2 \left(\frac{2\pi}{a_0}\right)^2 \left(\frac{\gamma_\kappa}{\alpha_\kappa^3}\right)(h_1^2 + h_2^2 + h_3^2)$$

$$+ i(k_BT)^2 \left(\frac{2\pi}{a_0}\right)^3 \left(\frac{\beta_\kappa}{\alpha_\kappa^3}\right) h_1 h_2 h_3$$

$$- (k_BT)^3 \left(\frac{2\pi}{a_0}\right)^4 \left(\frac{\gamma_\kappa}{\alpha_\kappa^4}\right)(h_1^2 + h_2^2 + h_3^2)^2$$

$$- (k_BT)^3 \left(\frac{2\pi}{a_0}\right)^4 \left(\frac{\delta_\kappa}{\alpha_\kappa^4}\right)(h_1^4 + h_2^4 + h_3^4$$

$$\left. - \tfrac{3}{5}[h_1^2 + h_2^2 + h_3^2]^2)\right\} \quad (4\cdot11)$$

with

$$N_\kappa = \left[1 - 15k_BT\left(\frac{\gamma_\kappa}{\alpha_\kappa^2}\right)\right]^{-1}.$$

For the harmonic crystal, $\beta_\kappa = \gamma_\kappa = \delta_\kappa = 0$ and (4·11) reduces to

$$\exp[-W_\kappa(\mathbf{Q})] = \exp\left[-\frac{Q^2 k_BT}{2\alpha_\kappa}\right] = \exp[-\tfrac{1}{2}Q^2\overline{u_\kappa^2}]$$

which is equivalent to equation (2·7). The additional terms which occur for the anharmonic crystal are either isotropic in reciprocal space and with magnitudes determined by the parameter γ_κ, or anisotropic in reciprocal space and with magnitudes determined by the parameters $\beta_\kappa, \delta_\kappa$.

Equation (4·11) does not give the dependence of the temperature factor on the temperature T explicitly, as $\alpha_\kappa, \beta_\kappa, \gamma_\kappa, \delta_\kappa$ will vary under the influence of thermal

expansion. The temperature variation for these potential parameters can be accounted for by using the 'quasi-harmonic approximation'.

4·3. Quasi-harmonic theory

If the crystal expands on heating, there is a softening of the force constants and a corresponding reduction in the frequencies $\omega_j(\mathbf{q})$ of the normal modes of vibration. It is usually assumed that the relative change in frequency $\Delta\omega/\omega$ is the same for each normal mode and is proportional to the relative change in volume $\Delta v/v$ of the crystal. Thus

$$\frac{\Delta\omega}{\omega} = -\gamma_G \frac{\Delta v}{v} = -\gamma_G \chi T. \qquad (4\cdot12)$$

where the proportionality constant γ_G is known as the Grüneisen constant and χ is the volume coefficient of expansion (Ziman, 1964).

For a crystal with harmonic interatomic forces, the frequencies of the normal modes appear as ω^{-2} in the expression for the temperature factor [see expression (2·9)]. We can allow, therefore, for the effect of thermal expansion on the mode frequencies by replacing $\dfrac{1}{\omega_j^2(\mathbf{q})}$ in (2·9) with

$$\frac{1}{\omega_{0j}^2(\mathbf{q})} + \frac{\partial}{\partial T}\left(\frac{1}{\omega_j^2(\mathbf{q})}\right) \Delta T,$$

which [from equation (4·12)] is

$$\frac{1}{\omega_{0j}^2(\mathbf{q})}(1 + 2\gamma_G \chi T),$$

where $\omega_{0j}(\mathbf{q})$ is the normal mode frequency in the absence of thermal expansion.

This is the modification of the harmonic Debye–Waller theory known as the 'quasi-harmonic theory'. The quasi-harmonic theory gives the same expression for the temperature factor as the harmonic theory, apart from an extra factor $1 + 2\gamma_G \chi T$:

$$T_k(\mathbf{Q})^{\text{quasi-harmonic}} = T_\kappa(\mathbf{Q})^{\text{harmonic}}(1 + 2\gamma_G \chi T).$$

In terms of the Einstein model, the same result follows by assuming that the potential parameter α_κ in equation (4·2) varies with temperature in accordance with

$$\frac{1}{\alpha_\kappa} = \frac{1}{\alpha_{0\kappa}}(1 + 2\gamma_G \chi T)$$

or

$$\alpha_\kappa = \alpha_{0\kappa}(1 - 2\gamma_G \chi T)$$

where $\alpha_{0\kappa}$ is the value of α_κ in the absence of expansion and it is assumed that $2\gamma_G \chi T \ll 1$. The anharmonic potential parameters, $\beta_\kappa, \gamma_\kappa, \delta_\kappa \ldots$ in equation (4·8), will also decrease as the neighbouring atoms move apart under thermal expansion, and we shall assume that the temperature dependence of these parameters is the same as for α_κ:

$$\alpha_\kappa/\alpha_{0\kappa} = \beta_\kappa/\beta_{0\kappa} = \gamma_\kappa/\gamma_{0\kappa} = \delta_\kappa/\delta_{0\kappa} = 1 - 2\gamma_G \chi T. \qquad (4\cdot14)$$

4·4. Comparison with coupled oscillator treatment

The explicit dependence on temperature of the temperature factor follows by combining equations (4·11) and (4·14). The resultant expression for $2W_\kappa$ can be compared with the results given by the coupled oscillator treatment of Maradudin & Flinn for a cubic monatomic solid, by putting $\beta_\kappa = 0$ in (4·11) and dropping the subscript κ. The Einstein treatment then leads to the following expression for the exponent of the Debye–Waller factor e^{-2W}:

$$2W = \left(\frac{2\pi}{a_0}\right)^2 (h_1^2 + h_2^2 + h_3^2) \left[\frac{1}{\alpha_0}\right] k_B T$$

$$+ \left(\frac{2\pi}{a_0}\right)^2 (h_1^2 + h_2^2 + h_3^2) \left[\frac{2\gamma_G\chi}{\alpha_0 k_B}\right](k_B T)^2$$

$$- \left(\frac{2\pi}{a_0}\right)^2 (h_1^2 + h_2^2 + h_3^2) \left[\frac{20\gamma_0}{\alpha_0^3}\right](k_B T)^2$$

$$+ \left(\frac{2\pi}{a_0}\right)^4 (h_1^2 + h_2^2 + h_3^2) \left[\frac{2\gamma_0}{\alpha_0^4}\right](k_B T)^3$$

$$- \left(\frac{2\pi}{a_0}\right)^4 (h_1^2 h_2^2 + h_2^2 h_3^2 + h_3^2 h_1^2 - \tfrac{1}{3}h_1^4$$

$$- \tfrac{1}{3}h_2^4 - \tfrac{1}{3}h_3^4)\left[\frac{12\delta_0}{5\alpha_0^4}\right](k_B T)^3 \qquad (4\cdot15)$$

where the quantities in square brackets are independent of temperature.

The first term of (4·15) is the harmonic contribution to $2W$; the second term is the thermal expansion correction to the harmonic contribution; the third and fourth terms represent isotropic, anharmonic contributions arising from the quartic component of the potential; and the last term is the anisotropic, quartic contribution to $2W$.

The same set of five terms is given in the equation (6·11) of Maradudin & Flinn's paper. The two expressions for $2W$ are nearly identical as regards the dependence of the individual terms on the temperature T and the Miller indices $h_1 h_2 h_3$. The only important difference in the two expressions lies in the interpretation of the temperature-independent quantities multiplying each term: in general, however, these quantities cannot be calculated directly and so must be treated as adjustable parameters in analysing the intensity data.

5. Calculation of structure factors for Einstein solid

For the elastic scattering of X-rays, the structure factor $F(\mathbf{Q})$ is calculated from the expression

$$F(\mathbf{Q}) = \sum_{\kappa=1}^{n} f_\kappa(\mathbf{Q}) T_\kappa(\mathbf{Q}) \exp(i\mathbf{Q}\cdot\mathbf{r}_\kappa), \qquad (5\cdot1)$$

where the summation is over the n atoms in the unit cell. $f_\kappa(\mathbf{Q})$ is the X-ray atomic scattering factor of the κth atom, and $T_\kappa(\mathbf{Q})$ is its temperature factor. $\mathbf{r}_\kappa$ is the radius vector from the origin of the unit cell to the equilibrium position of the atom.

The temperature factor in (5·1) is given by

$$T_\kappa(\mathbf{Q}) = \langle \exp(i\mathbf{Q}.\mathbf{u}_\kappa) \rangle \qquad (5·2)$$

where $\mathbf{u}_\kappa$ is the thermal displacement. In the harmonic approximation, (5·2) reduces to the Ott expression:

$$T_\kappa(\mathbf{Q}) = \exp\langle -\tfrac{1}{2}(\mathbf{Q}.\mathbf{u}_\kappa)^2 \rangle .$$

However, Dawson (1967a) has pointed out that, in the general anharmonic case, $T_\kappa(\mathbf{Q})$ is a complex quantity of the form

$$T_\kappa(\mathbf{Q}) = T_{c,\kappa}(\mathbf{Q}) + iT_{a,\kappa}(\mathbf{Q}) \qquad (5·3)$$

where $T_{c,\kappa}(\mathbf{Q})$ is centrosymmetric about the equilibrium position of atom κ and $T_{a,\kappa}(\mathbf{Q})$ is antisymmetric. By expanding (5·2), we find that the centrosymmetric portion of the temperature factor is given by

$$T_{c,\kappa}(\mathbf{Q}) = 1 - \tfrac{1}{2}\langle(\mathbf{Q}.\mathbf{u}_\kappa)^2\rangle + \tfrac{1}{24}\langle(\mathbf{Q}.\mathbf{u}_\kappa)^4\rangle$$
$$+ \text{ higher even-degree terms in } \mathbf{Q}.\mathbf{u}_\kappa ,$$

and the antisymmetric portion by

$$T_{a,\kappa}(\mathbf{Q}) = -\tfrac{1}{6}\langle(\mathbf{Q}.\mathbf{u}_\kappa)^3\rangle + \tfrac{1}{120}\langle(\mathbf{Q}.\mathbf{u}_\kappa)^5\rangle$$
$$+ \text{ higher odd-degree terms in } \mathbf{Q}.\mathbf{u}_\kappa .$$

The X-ray atomic scattering factor $f_\kappa(\mathbf{Q})$ can be subdivided in the same way into centrosymmetric and antisymmetric parts, and this subdivision has been exploited by Dawson (1967a,b,c,d) in the interpretation of X-ray measurements on diamond, silicon and germanium. We shall avoid this extra complication here by writing (5·1) in the equivalent form for neutron scattering. This is done by replacing $f_\kappa(\mathbf{Q})$ with the nuclear scattering length b_κ, which is a scalar quantity independent of $\mathbf{Q}$.

Substituting (5·3) into (5·1) and writing

$$F(\mathbf{Q}) \equiv A(\mathbf{Q}) + iB(\mathbf{Q}) ,$$

we have

$$A(\mathbf{Q}) = \sum_\kappa b_\kappa [T_{c,\kappa}(\mathbf{Q}) \cos(\mathbf{Q}.\mathbf{r}_\kappa)$$
$$- T_{a,\kappa}(\mathbf{Q}) \sin(\mathbf{Q}.\mathbf{r}_\kappa)]$$

and

$$B(\mathbf{Q}) = \sum_\kappa b_\kappa [T_{c,\kappa}(\mathbf{Q}) \sin(\mathbf{Q}.\mathbf{r}_\kappa)$$
$$+ T_{a,\kappa}(\mathbf{Q}) \cos(\mathbf{Q}.\mathbf{r}_\kappa)] . \qquad (5·4)$$

Equation (5·4) will be used to calculate the structure factors for a few standard structure types. $F(\mathbf{Q})$ will be determined first in terms of the centrosymmetric and antisymmetric components of the temperature factors of the n atoms in the unit cell; expressions for the $T_{c,\kappa}$'s and $T_{a,\kappa}$'s will then be inserted, using the results of § 4.

5·1. Rocksalt structure

The atomic coordinates (X = cation, Y = anion) are

$$\left.\begin{array}{l} \text{X: } 000 \quad \tfrac{1}{2}\tfrac{1}{2}0 \quad \tfrac{1}{2}0\tfrac{1}{2} \quad 0\tfrac{1}{2}\tfrac{1}{2} \\ \text{Y: } \tfrac{1}{2}\tfrac{1}{2}\tfrac{1}{2} \quad 00\tfrac{1}{2} \quad 0\tfrac{1}{2}0 \quad \tfrac{1}{2}00 \end{array}\right\} . \qquad (5·5)$$

The site symmetry of both ions is $m3m$, so that the centre of symmetry at each site requires that $T_{a,\kappa} = 0$ for X and Y. Moreover, the presence of a centre of symmetry at the origin of the unit cell requires that $B(\mathbf{Q}) = 0$ in equation (5·4), and so the structure-factor equation reduces to

$$F(\mathbf{Q}) = \sum_\kappa b_\kappa T_{c,\kappa}(\mathbf{Q}) \cos(\mathbf{Q}.\mathbf{r}_\kappa) .$$

Putting

$$\mathbf{Q}.\mathbf{r} = 2\pi(h_1 x_1' + h_2 x_2' + h_3 x_3')$$

where x_1', x_2', x_3' are the fractional coordinates in (5·5), and summing over the X and Y sites gives:

$$\left.\begin{array}{ll} F(\mathbf{Q}) \equiv F(h_1 h_2 h_3) = 4b_\text{X}T_{c,\text{X}} + 4b_\text{Y}T_{c,\text{Y}} & \dots h,k,l \text{ even} \\ \qquad\qquad = 4b_\text{X}T_{c,\text{X}} - 4b_\text{Y}T_{c,\text{Y}} & \dots h,k,l \text{ odd} \\ \qquad\qquad = 0 & \dots h,k,l \text{ mixed} \end{array}\right\} . \qquad (5·6)$$

Here b_X, b_Y are the scattering amplitudes of the X, Y ions and $T_{c,\text{X}}, T_{c,\text{Y}}$ are their (centrosymmetric) temperature factors.

$T_{c,\text{X}}$ and $T_{c,\text{Y}}$ are given by equation (4·11) with $\beta_\kappa = 0$. Thus

$$T_{c,\text{X}} = N_\text{X} \exp\left[-\frac{Q^2 k_B T}{2\alpha_\text{X}}\right]\left\{1 - 15k_B T\left(\frac{\gamma_\text{X}}{\alpha_\text{X}^2}\right)\right.$$
$$+ 10(k_B T)^2 \left(\frac{2\pi}{a_0}\right)^2 \left(\frac{\gamma_\text{X}}{\alpha_\text{X}^3}\right)(h_1^2 + h_2^2 + h_3^2)$$
$$- (k_B T)^3 \left(\frac{2\pi}{a_0}\right)^4 \left(\frac{\gamma_\text{X}}{\alpha_\text{X}^4}\right)(h_1^2 + h_2^2 + h_3^2)^2$$
$$- \tfrac{2}{3}(k_B T)^3 \left(\frac{2\pi}{a_0}\right)^4 \left(\frac{\delta_\text{X}}{\alpha_\text{X}^4}\right)(h_1^4 + h_2^4 + h_3^4)$$
$$\left. - 3h_1^2 h_2^2 - 3h_2^2 h_3^2 - 3h_3^2 h_1^2)\right\} , \qquad (5·7)$$

where

$$N_\text{X} = \left[1 - 15k_B T\left(\frac{\gamma_\text{X}}{\alpha_\text{X}^2}\right)\right]^{-1} .$$

$\alpha_\text{X}, \gamma_\text{X}, \delta_\text{X}$ are the parameters in the expression

$$V_\text{X}(u_1 u_2 u_3) = V_0 + \tfrac{1}{2}\alpha_\text{X}(u_1^2 + u_2^2 + u_3^2) + \gamma_\text{X}(u_1^2 + u_2^2 + u_3^2)^2$$
$$+ \delta_\text{X}(u_1^4 + u_2^4 + u_3^4 - \tfrac{3}{5}[u_1^2 + u_2^2 + u_3^2]^2) ,$$

which represents the expansion of the potential of the X ion in powers of the cartesian coordinates u_1, u_2, u_3 of the thermal displacement of the ion. The same equation (5·7) also applies to the Y ion with X replaced by Y throughout.

We can simplify (5·7) by noting that the term

$$R = 10(k_B T)^2 \left(\frac{2\pi}{a_0}\right)^2 \left(\frac{\gamma_\text{X}}{\alpha_\text{X}^3}\right)(h_1^2 + h_2^2 + h_3^2)$$

in the brackets { } is much larger than the term

$$S = (k_B T)^3 \left(\frac{2\pi}{a_0}\right)^4 \left(\frac{\gamma_\text{X}}{\alpha_\text{X}^4}\right)(h_1^2 + h_2^2 + h_3^2)^2$$

in the same brackets. Thus the ratio R/S

$$= \frac{\alpha_X}{k_B T} \cdot \frac{5a_0^2}{2\pi^2} \cdot \frac{1}{h_1^2 + h_2^2 + h_3^2}$$

$$= \frac{1}{\langle u_X^2 \rangle} \cdot \frac{5a_0^2}{2\pi^2} \cdot \frac{1}{h_1^2 + h_2^2 + h_3^2} .$$

For NaCl and KCl, the mean-square atomic displacement $\langle u^2 \rangle \sim 10^{-3} a_0^2$ at 20 °C, so that

$$R/S \gg 1$$

except at high temperatures and high values of $\sin \theta/\lambda$. Similarly, we can show (taking $\gamma_X \sim \delta_X$) that the term R is much greater than the last term

$$U = \tfrac{2}{3}(k_B T)^3 \left(\frac{2\pi}{a_0}\right)^4 \left(\frac{\delta_X}{a_X^4}\right) (h_1^4 + h_2^4 + h_3^4$$
$$- 3h_1^2 h_2^2 - 3h_2^2 h_3^2 - 3h_3^2 h_1^2)$$

in equation (5·7). R is a quadratic term in the components of Q and S, U are quartic terms; the same conclusion regarding the relative magnitudes of the quadratic and quartic terms is given by the coupled-oscillator treatments of Maradudin & Flinn (1963) and Kashiwase (1965).

Thus omitting the quartic terms from (5·7), and writing $e^{-x} \simeq 1 - x$ for $x \ll 1$, the temperature factor of the X ion is given approximately by

$$T_{c, X} = \exp \left[- \frac{Q^2 k_B T}{2\alpha_X} \left(1 - 20 k_B T \frac{\gamma_X}{\alpha_X^2}\right) \right]. \quad (5·7a)$$

In terms of the temperature-independent potential parameters, α_{0X} and γ_{0X}, this can be written [see equation (4·14)]

$$T_{c, X} = \exp \left[- \frac{k_B T}{2\alpha_{0X}} (1 + 2\chi \gamma_G T) \right.$$
$$\left. \times \left(1 - 20 k_B T \frac{\gamma_{0X}}{\alpha_{0X}^2}\right) Q^2 \right], \quad (5·8)$$
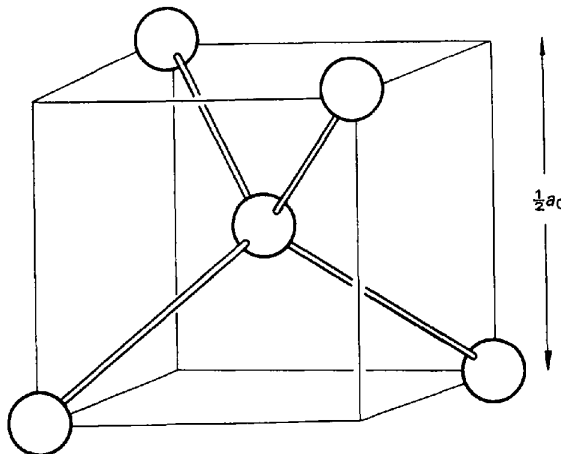

Fig. 5. Coordination of an atom in the diamond structure. Centres of symmetry are located half way between adjacent atoms but not at the atomic sites, so that the temperature factor has a non-vanishing antisymmetric component.

or

$$B_X(T) = \frac{8\pi^2 k_B T}{\alpha_{0X}} \left(1 + T \left[2\chi \gamma_G - 20 k_B \frac{\gamma_{0X}}{\alpha_{0X}^2}\right] \right.$$
$$\left. + \text{terms in } T^2, T^3 \dots \right) \quad (5·9)$$

where $B_X(T)$ is the isotropic B-factor of the X ion at temperature T, defined by

$$T_{c, X} = \exp \left(- B_X(T) \sin^2\theta/\lambda^2\right).$$

Equation (5·9) (with an identical equation for the Y ion) shows that the anharmonic contribution to the temperature factors of crystals with the rocksalt structure can be expressed approximately as an increase ΔB in the isotropic B-factors. ΔB for atom κ ($=$ X or Y) is

$$\Delta B_\kappa = B_\kappa^h . T[2\chi \gamma_G - 20 k_B \gamma_{0\kappa}/\alpha_{0\kappa}^2] \quad (5·10)$$

where the harmonic B-factor is

$$B_\kappa^h = 8\pi^2 k_B T/\alpha_{0\kappa} .$$

Thus, in the harmonic approximation, B_X and B_Y are proportional to temperature. In the anharmonic crystal, an extra term appears in the expression for the B-factor. This term is proportional to T^2 and is compounded of two parts: one due to thermal expansion and the other due to the quartic modification of the potential and representing the softening of the vibration at large amplitudes. Equations (5·9) and (5·10) will be used in § 6 to interpret experimental data recorded at different temperatures on KCl.

5·2. Diamond structure

There are eight identical atoms in the cubic unit cell, each tetrahedrally coordinated to its four nearest neighbours (Fig. 5). Choosing an origin at the centre of symmetry midway between two atoms, the atomic coordinates are:

$$\bar{7}\bar{7}\bar{7}_{888} \quad \bar{3}\bar{3}\bar{7}_{888} \quad \bar{3}\bar{7}\bar{3}_{888} \quad \bar{7}\bar{3}\bar{3}_{888} \quad (A \text{ sites})$$

and

$$\tfrac{1}{8}\tfrac{1}{8}\tfrac{1}{8} \quad \tfrac{5}{8}\tfrac{5}{8}\tfrac{1}{8} \quad \tfrac{5}{8}\tfrac{1}{8}\tfrac{5}{8} \quad \tfrac{1}{8}\tfrac{5}{8}\tfrac{5}{8} \quad (B \text{ sites}). \quad (5·11)$$

With this choice of origin, $B(Q) = 0$ in the structure-factor expression

$$F(Q) = A(Q) + iB(Q).$$

All atoms are at sites of cubic tetrahedral ($\bar{4}3m$) symmetry.

Inserting the coordinates (5·11) into (5·4) gives

$$F(h_1 h_2 h_3) = 8b \left[T_{c, A} \cos \left(\frac{7\pi}{4} (h_1 + h_2 + h_3)\right) \right.$$
$$\left. - T_{a, A} \sin \left(\frac{7\pi}{4} (h_1 + h_2 + h_3)\right) \right],$$

where b is the scattering amplitude, $T_{c, A}$ is the centrosymmetric component and $T_{a, A}$ is the antisymmetric component of the temperature factor of atoms on the A sublattice. The corresponding components, $T_{c, B}$ and

$T_{a,B}$, of the temperature factor for the B sublattice are related to $T_{c,A}$ and $T_{a,A}$ by

$$T_{c,B} = T_{c,A}, \quad T_{a,B} = -T_{a,A}.$$

The structure factors subdivide into four groups, depending on the value of the index sum, $h_1 + h_2 + h_3$. Thus

$$
\begin{aligned}
F(h_1 h_2 h_3) &= 8bT_{c,A} && \text{for } h_1 + h_2 + h_3 \\
&&& = 4n, \text{ group (i)}, \\
&= 8bT_{a,A} && \text{for } h_1 + h_2 + h_3 \\
&&& = 4n+2, \text{ group (ii)}, \\
&= 4\sqrt{2}b(T_{c,A} + T_{a,A}) && \text{for } h_1 + h_2 + h_3 \\
&&& = 4n+1, \text{ group (iii)}, \\
&= 4\sqrt{2}b(T_{c,A} - T_{a,A}) && \text{for } h_1 + h_2 + h_3 \\
&&& = 4n-1, \text{ group (iv)}.
\end{aligned}
\qquad (5 \cdot 12)
$$

Note that $T_{a,A} = 0$ for a harmonic crystal, so that the $4n+2$ reflexions are forbidden: they are not forbidden if anharmonic vibrations are taken into account. (In X-ray scattering, the presence of $4n+2$ reflexions can be associated with the antisymmetric component of the scattering amplitude, but there is no such component in neutron nuclear scattering.)

Explicit forms of $T_{c,A}$ and $T_{a,A}$ in equation (5·12) are derived from equation (4·11). The expansion of the potential function now includes a third-order term $\beta_A u_1 u_2 u_3$ —

$$V(u_1 u_2 u_3) = V_0 + \tfrac{1}{2}\alpha_A r^2 + \beta_A u_1 u_2 u_3$$
$$+ \text{ higher-order terms}$$

— and if higher-order terms are neglected ($\gamma = \delta \ldots = 0$), $T_{c,A}$ and $T_{a,A}$ are given by

$$
T_{c,A} = \exp\left(-\frac{Q^2 k_B T}{2\alpha_A}\right)
$$

and

$$
T_{a,A} = \exp\left(-\frac{Q^2 k_B T}{2\alpha_A}\right)(k_B T)^2 \left(\frac{2\pi}{a_0}\right)^3
$$
$$
\times \left(\frac{\beta_A}{\alpha_A^3}\right) h_1 h_2 h_3.
\qquad (5 \cdot 13)
$$

Equations (5·13) have been used by Dawson & Willis (1967) to calculate the intensities of reflexions in the groups (ii), (iii) and (iv) of (5·12); all these reflexions involve the third-order anharmonic parameter β_A. Some of their results are given in Fig.6, which shows the influence of temperature on the calculated intensities of 666 and 864 in group (ii), 755 in group (iii), and 177 and 933 in group (iv). The calculations relate to germanium: they indicate only qualitative behaviour as there is no experimental value available for β_A, which was assumed to be 10^{-11} erg A^{-3} and to be independent of temperature. The three reflexions 755, 177 and 933, sharing the same value of $h_1^2 + h_2^2 + h_3^2$, are equal in intensity for the harmonic crystal (broken line in Fig. 6). Anharmonic vibrations cause a deviation

of the intensities from the harmonic values. The deviation is largest for 755, because its diffraction vector is closest to the tetrahedral direction joining nearest neighbours, and is smallest for 177 whose diffraction vector is closest to [100]. The intensities of 666 and 864 in Fig.6 arise solely from the anharmonic contribution to the temperature factor.

5·3. Fluorite structure

In the rocksalt structure, the atomic site symmetry is $m3m$, so that there is no antisymmetric component of the temperature factors. The site symmetry is $\bar{4}3m$ in the diamond structure, and the antisymmetric component represents the most important anharmonic contribution to the temperature factor. Both types of site symmetry are present in the fluorite structure.

The atomic coordinates are

$$
\begin{aligned}
\text{X:} &\ 000 \quad 0\tfrac{1}{2}\tfrac{1}{2} \quad \tfrac{1}{2}0\tfrac{1}{2} \quad \tfrac{1}{2}\tfrac{1}{2}0 \\
\text{Y:} &\ \tfrac{1}{4}\tfrac{1}{4}\tfrac{1}{4} \quad \tfrac{1}{4}\tfrac{3}{4}\tfrac{3}{4} \quad \tfrac{3}{4}\tfrac{1}{4}\tfrac{3}{4} \quad \tfrac{3}{4}\tfrac{3}{4}\tfrac{1}{4} \\
\text{Y':} &\ \tfrac{3}{4}\tfrac{3}{4}\tfrac{3}{4} \quad \tfrac{3}{4}\tfrac{1}{4}\tfrac{1}{4} \quad \tfrac{1}{4}\tfrac{3}{4}\tfrac{1}{4} \quad \tfrac{1}{4}\tfrac{1}{4}\tfrac{3}{4}
\end{aligned}
\qquad (5 \cdot 14)
$$

where X refers to the cation positions and Y, Y' to the anion positions. Each cation is surrounded by eight anions at the corners of a cube and each anion by four cations at the corners of a regular tetrahedron (see Fig.7). X sites have $m3m$ symmetry and Y, Y' sites $\bar{4}3m$ symmetry.
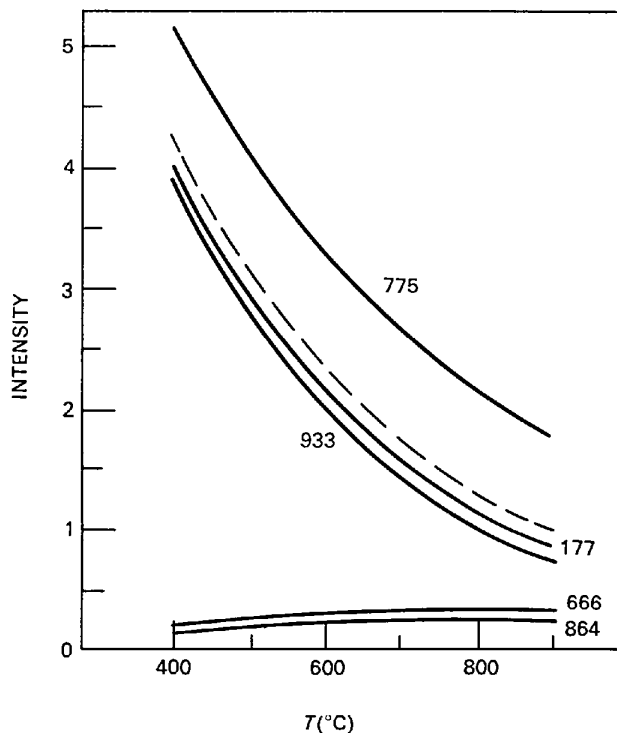

Fig.6. Variation with temperature of Bragg intensities of germanium, calculated assuming $\beta_A = 10^{-11}$ erg.Å^{-3}. The broken line gives the intensities of 755, 177 and 933 for $\beta_A = 0$ (after Dawson & Willis, 1967).

Putting the coordinates (5·14) into (5·4):

$$F(h_1h_2h_3) = 4b_X T_{c,X} + 8b_Y T_{c,Y} \text{ for } h_1+h_2+h_3 = 4n$$
$$= 4b_X T_{c,X} - 8b_Y T_{c,Y} \text{ for } h_1+h_2+h_3 = 4n+2$$
$$= 4b_X T_{c,X} - 8b_Y T_{a,Y} \text{ for } h_1+h_2+h_3 = 4n+1$$
$$= 4b_X T_{c,X} + 8b_Y T_{a,Y} \text{ for } h_1+h_2+h_3 = 4n-1.$$

$$(5·15)$$

b_X is the scattering amplitude of the cation, $T_{c,X}$ the centrosymmetric part and $T_{a,X}$ the antisymmetric part of the temperature factor of the cation, with similar quantities, $b_Y, T_{c,Y}, T_{a,Y}$, referring to the anion at a Y site. The relations

$$T_{a,X} = 0, \quad T_{c,Y} = T_{c,Y}', \quad T_{a,Y} = -T_{a,Y}'$$

have been used in deriving (5·15).

If the potential function $V(u_1u_2u_3)$ for both cation and anion is expanded up to the fourth power of the displacement, the temperature factors $T_{c,X}$ and $T_{c,Y}$ in (5·15) can be written from equation (5·7a) as:

CATION

ANION

Fig. 7. Coordination of anion and cation in fluorite structure.

$$T_{c,X} = \exp\left[-\frac{Q^2 k_B T}{2\alpha_X}\left(1 - 20k_B T\,\frac{\gamma_X}{\alpha_X^2}\right)\right]$$

and

$$T_{c,Y} = \exp\left[-\frac{Q^2 k_B T}{2\alpha_Y}\left(1 - 20k_B T\,\frac{\gamma_Y}{\alpha_Y^2}\right)\right].$$

$$(5·16)$$

The antisymmetric component $T_{a,Y}$ is given by the imaginary part of equation (4·11):

$$T_{a,Y} = \left(1 - 15k_B T\,\frac{\gamma_Y}{\alpha_Y^2}\right)^{-1}\exp\left[-\frac{Q^2 k_B T}{2\alpha_Y}\right]$$

$$\times \ (k_B T)^2\left(\frac{2\pi}{a_0}\right)^3\left(\frac{\beta_Y}{\alpha_Y^3}\right)h_1h_2h_3. \quad (5·17)$$

We have taken the potential for the cation as

$$V_X(u_1u_2u_3) = V_{0X} + \tfrac{1}{2}\alpha_X(u_1^2+u_2^2+u_3^2) + \gamma_X(u_1^2+u_2^2+u_3^2)^2,$$

and for the anion

$$V_Y(u_1u_2u_3) = V_{0Y} + \tfrac{1}{2}\alpha_Y(u_1^2+u_2^2+u_3^2)$$
$$+ \beta_Y u_1u_2u_3 + \gamma_Y(u_1^2+u_2^2+u_3^2)^2.$$

It is shown in the next section that the available experimental data on fluorite-type crystals can be interpreted satisfactorily from equations (5·15), (5·16) and (5·17), taking the quartic parameters, γ_X and γ_Y, as zero.

6. Experimental results

It is customary to use the Debye–Waller theory, based on the harmonic approximation, to account for the effect of thermal motion on the Bragg intensities. To assess the importance of the anharmonic modifications to the Debye–Waller theory, discussed in the earlier sections of Part B, observations are required over a range of temperatures, preferably on crystals with relatively simple structures. Unfortunately, observations of this kind are extremely few.

We choose the data of James & Brindley (1928) on KCl to analyse the influence of anharmonicity on the Debye–Waller factors determined with X-rays. These measurements, carried out forty years ago with an ionization chamber as detector, are still the most extensive measurements on a crystal with the rocksalt structure. They have been analysed by Kashiwase (1965), using the anharmonic theory based on the model of coupled oscillators, but we shall show that essentially the same results are given by an analysis based on the simpler approach described in § 4 and 5.

Suitable neutron studies at high temperatures are restricted largely to fluorite-type compounds. The most detailed observations relate to BaF_2, and the analysis of these is described in § 6·2.

6·1. Potassium chloride (X-rays)

James & Brindley examined the intensities of the 400, 600 and 800 Bragg reflexions in the temperature range 86–936 °K. Their experimental measurements, given in Table 1 of their paper, are reproduced here
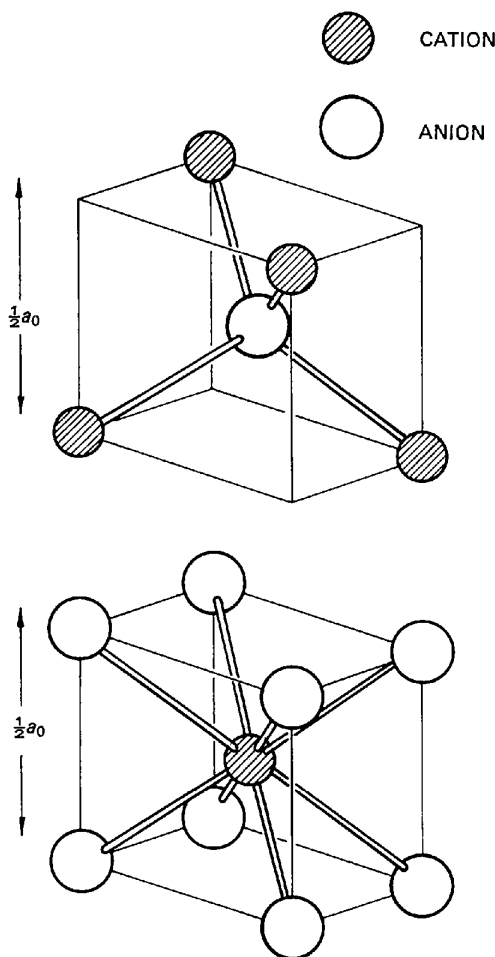
in the first three columns of Table 2. The second column in Table 2 lists the temperature T at which measurements were made of the integrated intensity $\varrho(T)$, and the third column gives the ratio $\varrho(T)/\varrho(T_0)$, where $\varrho(T_0)$ is the integrated intensity at the reference temperatuıe, T_0, of 290°K.

The intensities $\varrho(T)$ recorded by James & Brindley included a contribution from thermal diffuse scattering. The corrected intensities are

$$\varrho^{\text{corr}}(T)=\varrho(T)\div(1+\alpha)$$

where the correction factor for TDS is $1+\alpha$. The method of calculating α for KCl is described later, in § 9·1, and this procedure was used to derive the corrected ratio $\varrho^{\text{corr}}(T)/\varrho^{\text{ccrr}}(T_0)$ in the fifth column of Table 2.

The final column of the Table lists the quantity

$$\left(\frac{\lambda}{\sin\theta}\right)^2\ln[\varrho^{\text{corr}}(T)/\varrho^{\text{corr}}(T_0)]\,.$$

The Debye–Waller factor at temperature T is $\exp[-2B(T)\sin^2\theta/\lambda^2]$, so that this quantity is equivalent to

$$2[B(T)-B(T_0)]\,,$$

where, from equation (5·9),

$$B(T)=B^h(T)\left[1+T\left(2\chi\gamma_G-20k_B\frac{\gamma_0}{\alpha_0^2}\right)\right]\,. \quad (6\cdot1)$$

The masses of the K and Cl ions are sufficiently close to justify using the same B-factor for both ions, so that the subscript X can be dropped in the expression (5·9).

Theoretical values of the harmonic B-factors, $B^h(T)$ in (6·1), have been calculated recently by Buyers & Smith (1968) for the temperature range 0 to 900°K, using published data for the frequencies $\omega_j(\mathbf{q})$ and eigenvectors $\mathbf{e}_j(\mathbf{q})$ of KCl. The broken line A in Fig.8 corresponds to the harmonic theory, based on Buyers & Smith's calculations. Because of the effect of anharmonicity, the experimental points (closed circles) lie appreciably below this line.

Curve B in Fig.8 has been drawn using equation (6·1) in its quasi-harmonic form, that is, by retaining the thermal expansion term but writing

$$\frac{\gamma_0}{\alpha_0^2}=0\,.$$

Curve C represents the anharmonic form of equation (6·1) with

$$\frac{\gamma_0}{\alpha_0^2}=-0\cdot14\,.\,10^{12}\,\text{erg}^{-1}\,.$$

This latter value was chosen so as to make the anharmonic curve pass through the experimental points at the highest temperatures, where the influence of anharmonicity is greatest. The harmonic parameter α_0

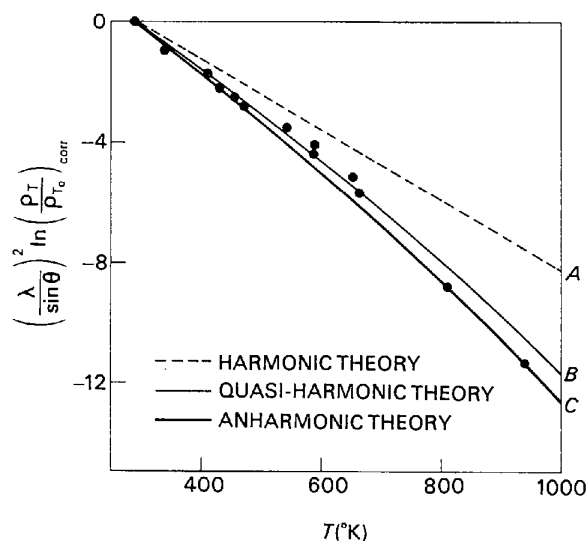Fig.8. The logarithm of the integrated intensities from KCl plotted against temperature. Experimental points of James & Brindley (1928) shown as closed circles. Curve A was calculated using the harmonic Debye–Waller theory; curve B was calculated using the quasi-harmonic theory, to include the effect of thermal expansion; curve C was calculated using the anharmonic theory, accounting for both thermal expansion and quartic anharmonicity.

Table 2. *X-ray measurements of James & Brindley*

Reflexion	T (°K)	$\frac{\varrho(T)}{\varrho(T_0)}$	$1+\alpha$	$\frac{\varrho^{\text{corr}}(T)}{\varrho^{\text{corr}}(T_0)}$	$\left(\frac{\lambda}{\sin\theta}\right)^2\ln\left(\frac{\varrho^{\text{corr}}(T)}{(\varrho^{\text{corr}}T_0)}\right)$
	290=(T_0)	1·00	1·03	1·00	0
	455	0·79	1·05	0·78	−2·46
400 (sin θ/λ=0·3211)	543	0·72	1·06	0·70	−3·46
	663	0·58	1·08	0·56	−5·69
	807	0·43	1·10	0·41	−8·77
	936	0·336	1·11	0·31	−11·33
	412	0·73	1·12	0·68	−1·69
600 (sin θ/λ=0·4819)	588	0·44	1·17	0·39	−4·09
	652	0·35	1·19	0·30	−5·14
	336	0·78	1·17	0·69	−0·91
800 (sin θ/λ=0·6426)	430	0·48	1·22	0·40	−2·19
	471	0·38	1·25	0·31	−2·80
	587	0·21	1·31	0·17	−4·36

is given by

$$\alpha_0 = 8\pi^2 k_B T / B^h(T)$$

which works out at about 2.10^{-12} erg Å^{-2}, so that the anharmonic parameter γ_0 is $0.6 \cdot 10^{-12}$ erg Å^{-4}. In calculating curves B and C in Fig. 8, the Grüneisen constant for KCl was taken from Slater (1939) and the mean expansion coefficient from Clark (1966).

Thermal expansion accounts for the bulk of the anharmonic contribution to the Debye–Waller factors, but there is also a small quartic contribution represented by the difference between curves B and C. This quartic term was ignored in the earlier analysis of James & Brindley's results by Paskin (1957). Its magnitude, calculated here for the Einstein model, is in good agreement with that calculated by Kashiwase (1965). However, a critical appraisal of the anharmonic theory requires more precise experimental data, such

as could be obtained, for example, by repeating James & Brindley's experiment using modern diffractometer techniques.

6·2. Barium fluoride (neutrons)

Accurate neutron diffraction data are available from measurements on compounds with the fluorite structure. A number of binary compounds have been examined at different temperatures, and Table 3 summarizes the compositions and temperature ranges covered.

For all the compounds in Table 3, systematic intensity differences have been observed between independent reflexions sharing the same value of $Q^2 (= 16\pi^2 \sin^2\theta/\lambda^2)$, and none of these observations can be explained by the harmonic (or quasi-harmonic) Debye–Waller theory. In the earlier work, the differences were accounted for in terms of a phenom-

Table 3. *Fluorite-type compounds examined with neutrons*

Compound	Temperature range	Reference
UO_2	4–1370°K	Willis (1963a,b)
		Willis & Taylor (1965)
		Dawson, Hurley & Maslen (1967)
		Rouse, Willis & Pryor (1968)
ThO_2	290–1370°K	Willis (1963a,b)
CaF_2	290– 770°K	Willis (1965)
		Dawson, Hurley & Maslen (1967)
CeO_2	290°K	Valentine & Willis (1965)
BaF_2	290– 870°K	Cooper, Rouse & Willis (1968)

Table 4. BaF_2: *observed values of* e^{-2W} *for odd-index reflexions*

(from Cooper et al., 1968)

$h_1h_2h_3$	$h_1^2+h_2^2+h_3^2$	20°C	88°C	159°C	239°C	317°C	398°C	596°C	$h_1h_2h_3$
511	} 27	0·75	0·76	0·72	0·63	0·61	0·55	0·46	{ 511
333		–	–	0·73	–	0·64	0·61	0·56	{ 333
711	} 51	0·63	0·60	0·54	0·46	0·41	0·34	0·24	{ 711
155		–	0·59	0·51	0·42	0·37	0·30	0·21	{ 155
355	59	–	0·60	0·52	0·45	0·41	0·35	0·27	355
733	67	0·56	0·52	0·46	0·38	0·34	0·28	0·20	733
555	75	0·48	0·41	0·32	0·24	0·18	0·12	0·058	555
911	83	0·48	0·43	0·35	0·27	0·21	0·16	0·087	911
933	}	0·39	0·33	0·25	0·17	0·13	0·089	0·040	{ 933
177	} 99	0·42	0·35	0·27	0·19	0·14	0·10	0·047	{ 177
755	}	0·45	0·41	0·34	0·26	0·22	0·17	0·098	{ 755
377	107	0·43	0·38	0·30	0·23	0·18	0·13	0·073	377
11, 1, 1	} 123	0·35	0·30	0·22	0·15	0·11	0·073	–	{ 11, 1, 1
577		0·29	0·22	0·15	0·092	0·060	0·036	–	{ 577

Table 5. BaF_2: *observed values of* e^{-2W} *for even-index reflexions*

(from Cooper et al., 1968)

$h_1h_2h_3$	$h_1^2+h_2^2+h_3^2$	20°C	88°C	159°C	239°C	317°C	398°C	596°C	$h_1h_2h_3$
222	12	–	–	0·71	0·64	0·61	–	0·47	222
600	} 36	0·51	0·47	0·39	0·30	0·24	0·18	0·080	{ 600
244		0·52	0·45	0·38	0·29	0·24	0·18	0·084	{ 244
622	44	0·45	0·39	0·30	0·23	0·17	0·12	0·041	622
644	68	0·28	0·21	0·15	0·090	0·056	0·031	–	644
266	76	0·24	0·19	0·12	0·065	0·037	0·018	–	266
10, 0, 0	100	0·15	0·095	0·050	0·019	–	–	–	10, 0, 0
666	} 108	0·13	0·080	0·040	–	–	–	–	{ 666
10, 2, 2		0·12	0·078	0·040	–	–	–	–	{ 10, 2, 2

enological theory, in which the anion at $\frac{1}{4}\frac{1}{4}\frac{1}{4}$ is replaced by four '$\frac{1}{4}$-anions' with coordinates $\frac{1}{4}+\delta$ $\frac{1}{4}+\delta$ $\frac{1}{4}+\delta$, $\frac{1}{4}+\delta$ $\frac{1}{4}-\delta$ $\frac{1}{4}-\delta$, $\frac{1}{4}-\delta$ $\frac{1}{4}+\delta$ $\frac{1}{4}-\delta$, $\frac{1}{4}-\delta$ $\frac{1}{4}-\delta$ $\frac{1}{4}+\delta$. δ is a kind of anharmonic parameter related to the thermal displacement of the anion. The diffraction data in the later work were interpreted by means of the anharmonic theory based on the Einstein model. The most comprehensive study to date is that on BaF_2, and we shall show that this anharmonic theory, as described in §§ 4 and 5, gives a complete account of all the experimental measurements on this compound.

The observed Debye–Waller factors, e^{-2W}, expressing the reduction in the Bragg intensities caused by thermal motion, are given in Tables 4 and 5 for odd-index and even-index reflexions of BaF_2. All these observations have been corrected for the contribution of thermal diffuse scattering (§ 9·2). At 20 °C the intensity of the 11,1,1 reflexion is 20% greater than the intensity of 577, and at 398 °C 11,1,1 has *twice* the intensity of 577: according to the harmonic Debye–Waller theory, the calculated structure factors are the same for both reflexions, and so the intensities should be equal at all temperatures. Similar intensity differences exist between odd-index reflexions in other groups with the same Q^2 (e.g. 933, 177 and 755, or 711 and 155; see Table 4). Moreover, the stronger intensities are associated with reflexions of the type

$$h_1+h_2+h_3=4n+1$$

and the weaker intensities with

$$h_1+h_2+h_3=4n-1 .$$

There is no noticeable splitting of the intensities in even-index groups with the same Q^2 (e.g. 666 and 10 2 2 or 600 and 244; see Table 5).

From § 5·3, the principal anharmonic modification of the intensities arises from the third-order anharmonic parameter, β_Y, characterizing the antisymmetric part $T_{a,Y}$ of the temperature factor of the fluorine anion. This antisymmetry causes a splitting of the intensities of odd-index reflexions with the same Q^2, but produces no splitting of the intensities within even-index groups [equation (5·15)].

The BaF_2 intensities were analysed by Cooper et al. (1968) using equations (5·15), (5·16) and (5·17), assuming the quartic parameters to be zero. The final R value obtained at all temperatures was about 1%, which is close to the limit set by the accuracy of the observations. Thus three potential parameters only, viz. the temperature-independent parameters $\alpha_{0\kappa}$ for barium and $\alpha_{0\kappa}, \beta_{0\kappa}$ for fluorine, were sufficient to account for the intensity measurements recorded at *all* temperatures. Taking the Grüneisen constant as 2·1, these parameters worked out as

$$\left. \begin{array}{l} \alpha_{0,Ba} = \quad 5\cdot54 . 10^{12} \text{ erg } \text{Å}^{-2} \\ \alpha_{0,F} = \quad 3\cdot59 . 10^{12} \text{ erg } \text{Å}^{-2} \\ \beta_{0,F} = -3\cdot48 . 10^{12} \text{ erg } \text{Å}^{-3} \end{array} \right\} . \qquad (6\cdot2)$$

The negative sign for $\beta_{0,F}$ implies that the amplitude of vibration of the fluorine ion is least along the $[\bar{1}\bar{1}\bar{1}]$ direction towards the nearest barium ion and greatest along the $[111]$ direction pointing towards an open position in the fluorite structure. The observed Bragg intensities could be accounted for completely by equation (5·15), with

$$\left. \begin{array}{l} b_X = b_{BA}(=0\cdot52 . 10^{-12} \text{ cm}) , \\ b_Y = b_F(=0\cdot56 . 10^{-12} \text{ cm}) , \\ T_{c,X} = \exp\left[-\dfrac{k_B T}{2\alpha_{BA}} Q^2\right] , \\ T_{c,Y} = \exp\left[-\dfrac{k_B T}{2\alpha_F} Q^2\right] \\ \text{and} \\ T_{a,Y} = \left(\dfrac{2\pi}{a_0}\right)^3 \dfrac{\beta_F}{\alpha_F^3} (k_B T)^2 h_1 h_2 h_3 \\ \qquad\qquad \times \exp\left[-\dfrac{Q^2 k_B T}{2\alpha_F}\right] , \end{array} \right\} \qquad (6\cdot3)$$

where

$$\alpha_{Ba}/\alpha_{0,Ba} = \alpha_F/\alpha_{0,F} = \beta_F/\beta_{0,F} = 1 - 2\chi\gamma_G T$$

and $\alpha_{0,Ba}$, $\alpha_{0,F}$, $\beta_{0,F}$ are given by (6·2). $a_0 = 6\cdot20$ Å at 20 °C and $\chi = 8\cdot7 . 10^{-5}$ °C^{-1}.

In the absence of thermal motion, the structure factors reduce to

$$\left. \begin{array}{ll} F'(h_1 h_2 h_3) = 4b_{Ba} + 8b_F & \text{for } h_1+h_2+h_3 = 4n \\ \qquad = 4b_{Ba} - 8b_F & \text{for } h_1+h_2+h_3 = 4n+2 \\ \qquad = 4b_{Ba} & \text{for } h_1+h_2+h_3 = 4n \pm 1 \end{array} \right\} . \qquad (6\cdot4)$$
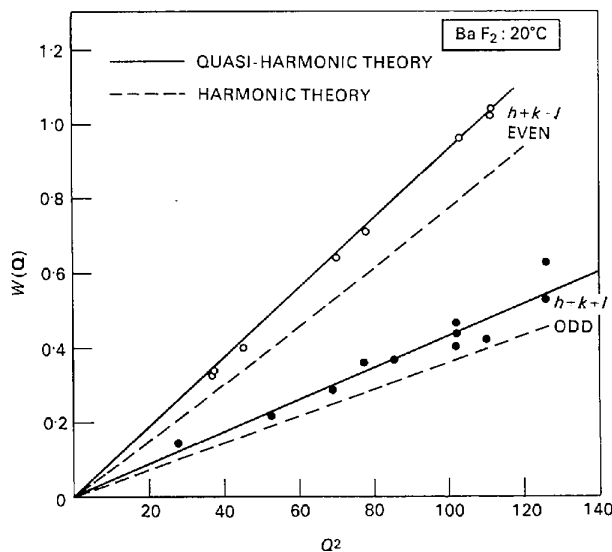

Fig. 9. BaF_2 at 20 °C; plot of $W(Q)$ *versus* Q^2. Experimental points for odd-index reflexions shown as closed circles, and for even-index reflexions as open circles. In the harmonic approximation $W(Q)$ is proportional to Q^2.

The calculated Debye–Waller factors, therefore, are

$$e^{-2W(Q)} = \left(\frac{F(h_1 h_2 h_3)}{F'(h_1 h_2 h_3)} \right)^2,$$

where $F(h_1 h_2 h_3)$ is obtained from equation (5·15) and (6·3) and $F'(h_1 h_2 h_3)$ from (6·4).

Figs. 9 and 10 are plots of $W(Q)$ *versus* Q^2 at 20 °C and at 398 °C respectively. The experimental observations were taken from Tables 4 and 5, and the theoretical curves were calculated using the quasi-harmonic theory (full lines: equations (6·3) with $\beta_F = 0$) and the harmonic theory (broken lines: equation (6·3) with $\beta_F = 0$ and $\chi = 0$). Neither theory can explain the odd-index data, but the quasi-harmonic treatment accounts satisfactorily for the Q-dependence of the even-index intenities.

Plots of $W(Q)$ *versus* temperature for a few odd-index and even-index reflexions are illustrated in Figs. 11 and 12. The quasi-harmonic theory underestimates the Debye–Waller factors of the 577 reflexion, Fig. 11(a), and overestimates the Debye–Waller factors of 733, Fig. 11(b). The anharmonic theory accounts for the temperature-dependence of both odd-index (Fig. 11) and even-index (Fig. 12) intensities. The chain-dotted
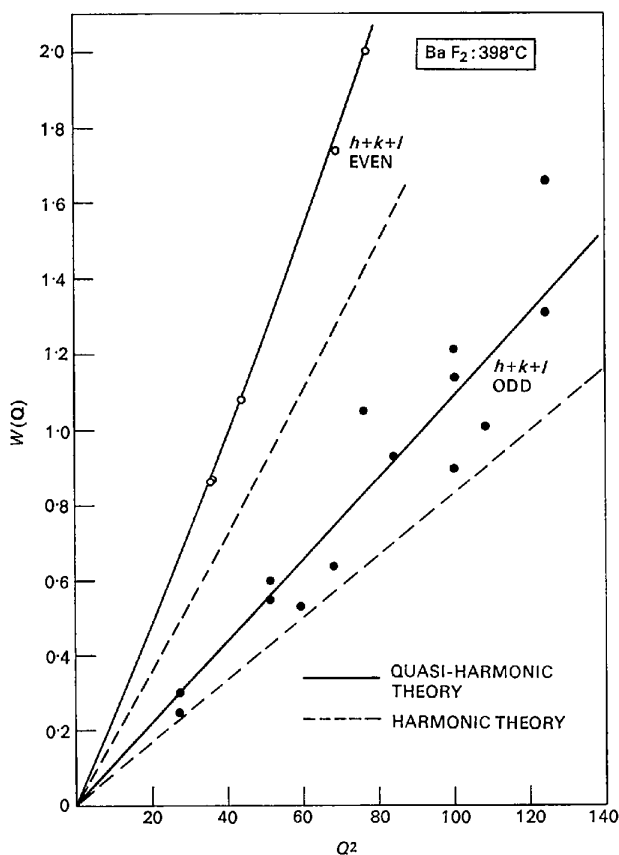
line in Figs. 11 and 12 indicates the Debye characteristic temperature, below which the classical theory breaks down.

We conclude from § 6 that anharmonic effects must be taken into account in the interpretation of accurate diffraction measurements. These effects are especially important for atoms occupying sites which are not centres of symmetry: in the case of BaF_2 at 20 °C, the observed intensities differ by up to 20% from the values predicted by the (quasi-harmonic) Debye–Waller theory, and the discrepancy increases to 90% at 400 °C. Anharmonic effects are accounted for satisfactorily by using an Einstein model of the crystal. The temperature factor can be expressed as the sum of a centrosymmetric part and an antisymmetric part

$$T_\kappa(Q) = T_{c,\kappa}(Q) + iT_{a,\kappa}(Q),$$

and explicit versions of $T_{c,\kappa}$ and $T_{a,\kappa}$ are derived by adopting a single-atom potential appropriate to the point symmetry of the site occupied by the atom κ. For non-cubic symmetries, it may be necessary to use a poor approximation to the potential function, but if there is no centre of symmetry at the atomic site (as is generally the case) any approximation to $T_{a,\kappa}$ is better than the Debye–Waller theory which always gives $T_{a,\kappa} = 0$.

C. EFFECT OF THERMAL DIFFUSE SCATTERING ON THE MEASURED INTENSITIES

Thermal diffuse scattering (TDS) of X-rays or neutrons constitutes an important part of the background in a diffraction pattern. This diffuse scattering peaks at the same positions as the Bragg reflexions, and can lead to errors in the measured intensities (see Fig. 1). We shall see that the errors are unlikely to exceed 25% under normal circumstances: they can be calculated sufficiently well using the formulae (given in § 2) based on the harmonic approximation.

The TDS close to the Bragg positions arises principally from first-order (one-phonon) scattering associated with the acoustic modes of vibration, and we shall assume that all other modes and higher-order processes can be ignored. It is implied in the following sections that the intensities are measured with a counter detector of fixed aperture, and that the Bragg intensity is estimated from the difference between the integrated intensity over the peak and the background intensity at the sides of the peak. The TDS correction for X-ray intensities measured by means of a photographic film is similar to that for a counter detector: for further discussion, see Annaka (1962).

Fig. 10. BaF_2 at 398 °C: plot of $W(Q)$ *versus* Q^2. Experimental points for odd-index reflexions shown as closed circles, and for even-index reflexions as open circles. In the harmonic approximation $W(Q)$ is proportional to Q^2.

7. Theory (X-rays)

The differential scattering cross-section, associated with first-order scattering involving the three acoustic modes of wave-vector q, is given by equation (2·10a). For such

low-energy modes (small $\mathbf{q}$), q is proportional to the frequency $\omega_j(\mathbf{q})$, or

$$\omega_j(\mathbf{q}) = |\mathbf{V}_j|q \qquad (7.1)$$

where $j = 1, 2, 3$ and $\mathbf{V}_j$ is the velocity of the mode with polarization state j. Substituting (7.1) into (2.10a):

$$\left(\frac{d\sigma(\mathbf{q})}{d\Omega}\right)_1 = \frac{NQ^2}{mq^2} |F(\mathbf{Q})|^2 \sum_{j=1}^{3} \frac{E_j(\mathbf{q}) \cos^2\alpha_j(\mathbf{q})}{V_j^2} . \qquad (7.2)$$

The total first-order intensity is obtained by integrating (7.2) over all the acoustic waves 'seen' by the detector during the scan across the Bragg reflexion. The scattering vector $\mathbf{Q}$ coincides with the reciprocal lattice vector $\mathbf{B}$ at the Bragg peak, so that, as a consequence of the momentum conservation rule

$$\mathbf{Q} + \mathbf{q} = \mathbf{B}$$

for first-order scattering, smaller q values are seen by the detector at the central part of the scan than at the extreme positions. For this reason, the q^{-2} dependence of the intensity in (7.2) gives rise to a TDS peak coincident with the zero-order Bragg peak.

7.1. Spherical approximation

The volume of reciprocal space seen by the detector is approximately a parallelipiped, whose dimensions depend on the solid angle subtended at the crystal and on the type of scan [see Figs. 13(b) and 13(c)]. The proper calculation of the TDS correction is rather complicated, but a rough estimate of its magnitude can be derived by taking a sphere of radius q_{max}, centred on the appropriate reciprocal lattice point, as the volume seen by the detector [Fig. 13(a)].

The experimental determination of the Bragg intensity requires combining the integrated intensity, recorded during the scan across the Bragg peak, with the background intensity at the sides of the peak. We must obtain expressions, therefore, for the first-order TDS intensity E_1^p which is included in the peak measurement, and for the first-order TDS intensity E_1^b included in the background measurement.

E_1^p is given by

$$E_1^p = \iint \left(\frac{d\sigma(\mathbf{q})}{d\Omega}\right)_1 dt\,d\Omega$$

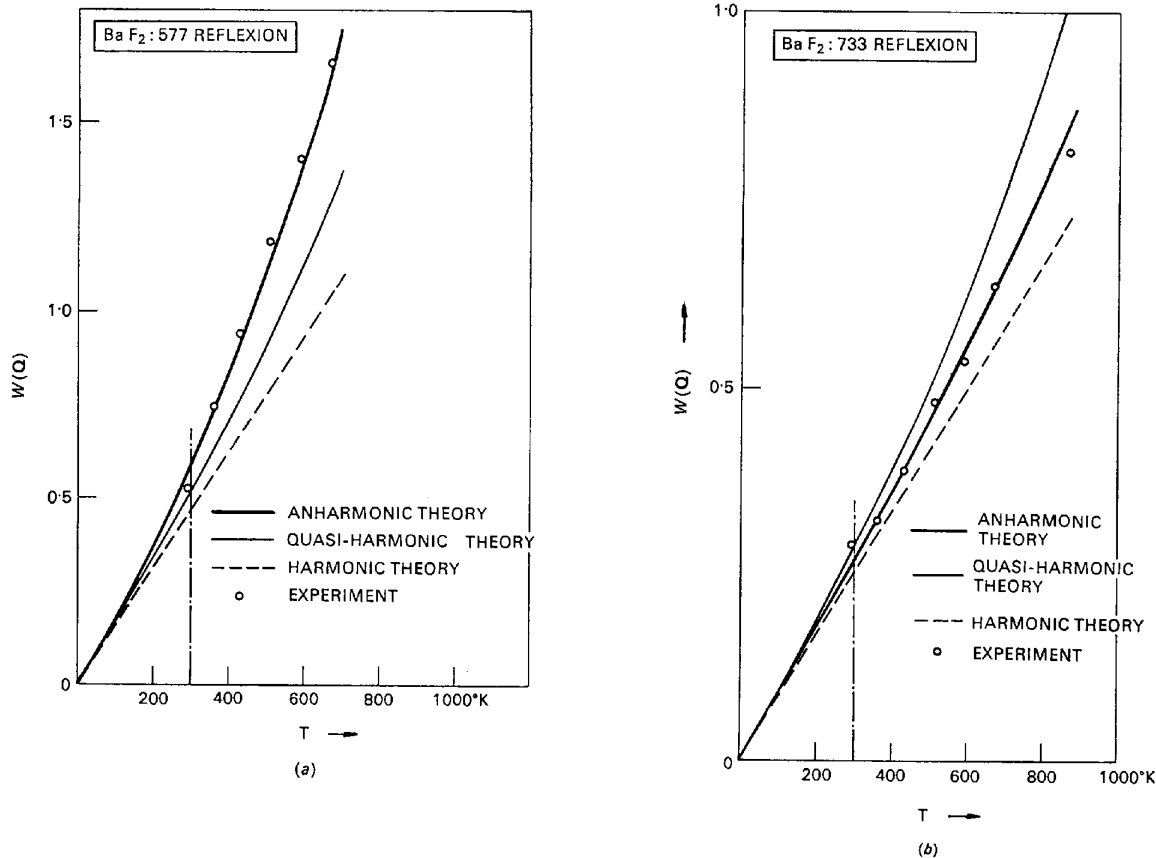where the integration is over time t and solid angle Ω.

Fig. 11. BaF$_2$: $W(\mathbf{Q})$ *versus* temperature for (a) 577 reflexion (b) 733 reflexion. In the harmonic approximation $W(\mathbf{Q})$ is proportional to T.
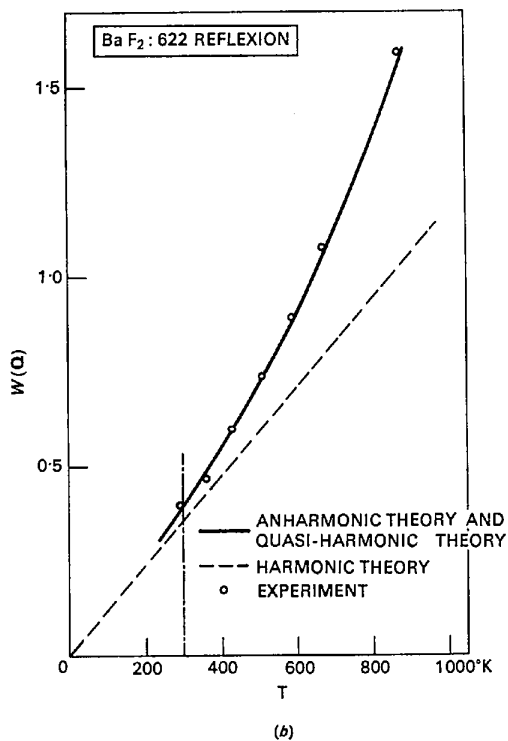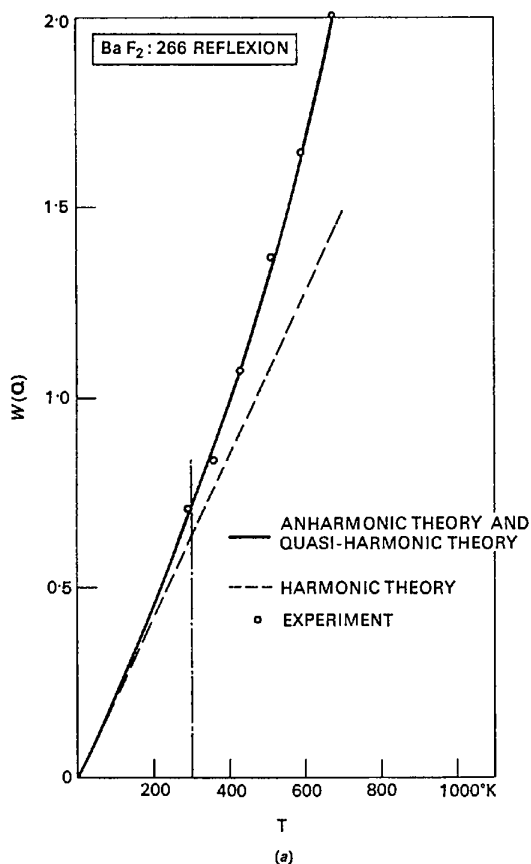
Fig. 12. BaF_2: $W(Q)$ versus temperature for (a) 266 reflexion (b) 622 reflexion. In the harmonic approximation $W(Q)$ is proportional to T.

Thus

$$E_1^p \omega = \iint \left(\frac{d\sigma(\mathbf{q})}{d\Omega}\right)_1 d\theta d\Omega$$

$$= \int_0^{q_{max}} \left(\frac{d\sigma(\mathbf{q})}{d\Omega}\right)_1 4\pi q^2 dq \frac{\lambda^3}{8\pi^3 \sin 2\theta} \quad (7\cdot3)$$

where ω is the angular velocity of the crystal. The term $(\lambda/2\pi)^3 \operatorname{cosec} 2\theta$ in (7·3) is the familiar Jacobian relating the angular co-ordinates θ, Ω with the cartesian co-ordinates in reciprocal space. Combining (7·2) and (7·3):

$$E_1^p \omega = \frac{NQ^2 |F(\mathbf{Q})|^2 \lambda^3 q_{max}}{2\pi^2 m \sin 2\theta_B}$$

$$\times \left\langle \sum_{j=1}^{3} \frac{E_j(\mathbf{q})\cos^2\alpha_j(\mathbf{q})}{V_j^2} \right\rangle \quad (7\cdot4)$$

where the brackets $\langle \rangle$ indicate the average value over all the $\mathbf{q}$ vectors contributing to the TDS. The first-order scattering is sufficiently close to the Bragg position to justify using $\theta = \theta_B$ in (7·4). The symbol $Q(=4\pi \sin \theta/\lambda)$ is not to be confused with the quantity proportional to $\lambda^3 |F(\mathbf{Q})|^2 \operatorname{cosec} 2\theta$ which is frequently denoted by Q also.

The integrated first-order TDS intensity included in the (normalized) background measurement, E_1^b, is less than E_1^p. Assuming that the acoustic modes associated with E_1^b have wave vectors whose average magnitude is q_{max}, we can write [cf. equation (7·3)]:

$$E_1^b \omega = \left(\frac{d\sigma(\mathbf{q})}{d\Omega}\right)_1 \int_0^{q_{max}} 4\pi q^2 dq \frac{\lambda^3}{8\pi^3 \sin 2\theta_B}$$

where $\left(\dfrac{d\sigma(\mathbf{q})}{d\Omega}\right)_1$ is evaluated, using equation (7·2), at $q = q_{max}$. The result is that E_1^b works out as one-third of the first-order peak intensity:

$$E_1^b = \tfrac{1}{3} E_1^p. \quad (7\cdot5)$$

The background is measured at a point where there is no Bragg (zero-order) intensity, i.e. $E_0^b = 0$. The integrated Bragg intensity included in the peak scan is

$$E_0^p = \iint \left(\frac{d\sigma}{d\Omega}\right)_0 dt d\Omega$$

or

$$E_0^p \omega = \left(\frac{\lambda}{2\pi}\right)^3 \operatorname{cosec} 2\theta_B \iiint \left(\frac{d\sigma}{d\Omega}\right)_0 dx_1 dx_2 dx_3$$

where $x_1 x_2 x_3$ are cartesian coordinates in reciprocal space. Inserting the zero-order cross section, $\left(\dfrac{d\sigma}{d\Omega}\right)_0$, from equation (2·5) gives

$$E_0^p \omega = \left(\frac{\lambda}{2\pi}\right)^3 \operatorname{cosec} 2\theta_B v_z N |F(\mathbf{Q})|^2. \quad (7\cdot6)$$

Combining (7·4), (7·5) and (7·6) we have finally

$$\frac{E_1^p - E_1^b}{E_0^p} = \frac{I_{TDS}}{I_{Bragg}} = \frac{8\pi}{3} \frac{Q^2 q_{max}}{mv_z}$$

$$\times \left\langle \sum_j \frac{E_j(\mathbf{q}) \cos^2\alpha_j(\mathbf{q})}{V_j^2} \right\rangle,$$

where I_{TDS} is the first-order TDS intensity included in the measured integrated intensity, I_{obs}, and I_{Bragg} is the zero-order intensity. Thus I_{obs} exceeds I_{Bragg} by a factor $1 + \alpha$,

$$I_{obs} = I_{Bragg}(1 + \alpha), \qquad (7·7)$$

where

$$\alpha = \frac{8\pi}{3} \frac{Q^2 q_{max}}{mv_z} \left\langle \sum_j \frac{E_j(\mathbf{q}) \cos^2\alpha_j(\mathbf{q})}{V_j^2} \right\rangle. \qquad (7·8)$$

This expression can be simplified at high temperatures ($T >$ Debye temperature) by replacing the mode energy $E_j(\mathbf{q})$ with $k_B T$. If we assume further that the acoustic modes propagate isotropically, one with longitudinal velocity V_l and two with transverse velocity V_t, equation (7·8) reduces to

$$\alpha = \frac{8\pi}{3} \frac{Q^2 q_{max}}{mv_z} k_B T \cdot \frac{1}{3} \left(\frac{1}{V_l^2} + \frac{2}{V_t^2} \right). \qquad (7·9)$$

This shows that (for a fixed value of q_{max}) α is proportional to Q^2, so that if α is sufficiently small to justify the replacement of $1 + \alpha$ by e^α, the effect of including TDS in the estimate of the Bragg intensity is to decrease artificially the overall B-factor. This decrease, ΔB, is given by

$$\alpha = 2\Delta B \sin^2\theta_B/\lambda^2 = (Q^2/8\pi^2)\Delta B \qquad [7·9(a)]$$

or

$$\Delta B = \frac{64\pi^3}{9} \frac{q_{max} k_B T}{mv_z} \left(\frac{1}{V_l^2} + \frac{2}{V_t^2} \right). \qquad (7·10)$$

In the more exact treatment of the TDS correction discussed in sections 7·2 and 7·3 below, the effective value of q_{max} in (7·10) varies with the Bragg angle θ_B. Thus the inclusion of TDS in the measurement of the integrated intensity cannot be compensated for properly by decreasing the B-factor: even if no particular interest attaches to the B-factor, it is preferable to correct the individual intensity measurements before treating B as an adjustable parameter in the analysis of the diffraction data.

7·2. Nilsson treatment

Nilsson (1957) has evaluated the correction term α for the case of a cubic crystal in which the intensities are measured by means of an ω-scan. In this scan, the detector is kept stationary at $\theta = \theta_B$ while the crystal rotates uniformly through the reflecting position. The volume swept out in reciprocal space during the scan

is illustrated in Fig. 13(b), where ab corresponds to the angular width of the detector aperture in the horizontal plane, normal to the rotation axis, and bc corresponds to the crystal oscillation angle: the total volume is proportional to the area $abcd$ multiplied by the vertical aperture of the detector.

Nilsson's expression for α, valid in the classical limit, is

$$\alpha = \sigma \cdot \frac{Q^2 \sin 2\theta_B k_B T}{12\pi\lambda} K. \qquad (7·11)$$

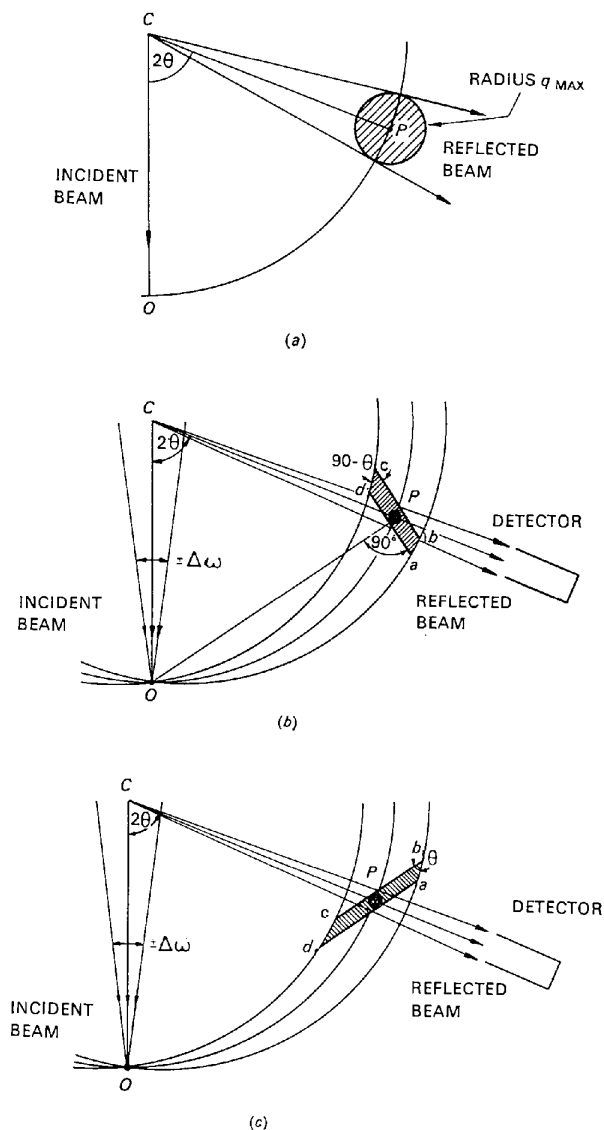K is related to the cubic elastic constants c_{11}, c_{12}, c_{44} by

Fig. 13. Volumes swept out in reciprocal space during the scan across the Bragg peak: (a) spherical approximation, (b) ω-scan, (c) $\theta/2\text{-}\theta$ scan. C is the centre of the Ewald sphere, O the origin of reciprocal space, and P the reciprocal lattice point.

$K = \frac{1}{5}(c_{11} - c_{12} - 2c_{44})\ (c_{11} + c_{12}) + c_{44}(2c_{11} + c_{44})/$

$\frac{1}{105}(c_{11} - c_{12} - 2c_{44})^2(c_{11} + 2c_{12} + c_{33})$

$+ \frac{1}{5}(c_{11} - c_{12} - 2c_{44})\ (c_{11} + c_{12})c_{44} + c_{11}c_{44}^2 ,$ (7·12)

and if the elastic waves propagate isotropically, (7·12) reduces to

$$K = \frac{2}{c_{44}} + \frac{1}{c_{11}} .$$

σ in (7·11) is an integral of the first-order TDS intensity over the volume scanned in reciprocal space. Nilsson assumes that the detector aperture is of infinite height in the vertical plane, and σ then reduces to an analytic expression [Nilsson's equation (8)] involving the oscillation angle and the horizontal width of the detector aperture. It is not difficult to show that Nilsson's expression for σ is equivalent to that given in equation (7·11) for the spherical approximation, apart from an angular-dependent factor which does not appear in the more approximate treatment.

7·3. Cooper–Rouse treatment

Nilsson's analysis has been developed further by Cooper & Rouse (Cooper & Rouse, 1968; Cooper, 1969). Nilsson's formula for α includes the quantity K, dependent on the elastic constants of the crystal, and the quantity σ, which is related to the oscillation angle and the detector aperture but is independent of the properties of the crystal. Cooper & Rouse have improved the derivation of σ in two ways: by avoiding the assumption of an infinite height of the detector aperture, and by extending the calculation to include the cases of both the ω-scan and the $\omega/2\theta$-, or $\theta/2\theta$-scan. In the $\theta/2\theta$-scan the detector moves at twice the angular velocity of the crystal, and the volume swept out in reciprocal space is as shown in Fig. 13(c), where ab represents the detector aperture, and bc the oscillation angle of the detector. σ is evaluated over the correct height of the aperture, using numerical methods for the integration of the first-order intensity over reciprocal space.

The Cooper–Rouse analysis constitutes the most reliable procedure available for correcting Bragg intensity measurements from a cubic crystal, made with either the ω-scan or the $\theta/2\theta$-scan, for the contribution of first-order thermal diffuse scattering. The analysis includes a number of cumbersome expressions involving the dimensions of the detector aperture, the oscillation range and the cubic elastic constants of the crystal, but provided these quantities are known, the TDS correction is obtained readily by a computer program.

The Cooper–Rouse treatment assumes that the TDS correction is isotropic in reciprocal space, depending on the magnitude of $\mathbf{Q}$ but not on its direction. This is a good approximation for most cubic crystals, but is much less satisfactory for non-cubic crystals. The evaluation of the anisotropic TDS correction for both cubic and non-cubic crystals constitutes a straightfor-

ward extension of the Cooper–Rouse analysis, and is described by Rouse, Willis & Cooper (1969).

8. Theory (neutrons)

The first-order scattering cross-section for slow neutrons is quoted in equation (2·13). The formula applies to the scattering by the $3n$ normal modes with the same wave vector $\mathbf{q}$; these modes must satisfy the conservation rules for momentum and energy given in equation (2·12). The total first-order intensity is obtained by integrating (2·13) over all those acoustic modes which are seen by the detector during the scan across the Bragg reflexion and which lie along the scattering surfaces defined by the conservation rules. In the X-ray case, there is only one scattering surface (the Ewald sphere); for one-phonon neutron scattering, the phonon energy is comparable with the neutron energy so that the situation is more complicated, and there are distinct scattering surfaces for phonon emission and phonon absorption, as well as for the different branches of the dispersion curves.

The neutron scattering surfaces change in both shape and position in reciprocal space as the crystal rotates. Seeger & Teller (1942) have shown that they can be represented approximately as ellipsoids or hyperboloids, depending on whether the incident neutrons are slower or faster than the velocity of sound in the crystal. These two cases must be examined separately.

8·1. Faster-than-sound neutrons

The scattering surface is a hyperboloid of two sheets, with the Ewald sphere lying between the sheets. The phonon-absorption process [− sign in equation (2·13)] corresponds to scattering involving $\mathbf{q}$ vectors terminating on one sheet, and phonon emission [+ sign in (2·13)] to scattering involving $\mathbf{q}$ vectors terminating on the other sheet. It turns out (Cochran, 1963) that the sum of the two cross-sections, assuming that $J_j = 1$ in (2·13), is equivalent (as $q \to 0$) to the cross-section given by the X-ray formula (2·10). The problem of calculating the first-order TDS correction is the same, therefore, as for X-rays and the formulae given in § 7 can be used.

8·2. Slower-than-sound neutrons

The scattering surface is an ellipsoid with the nearest reciprocal lattice point at one focus. The scattering is accompanied by phonon absorption alone when the crystal setting is on one side of the Bragg position, and by phonon emission alone when the setting is on the other side of the Bragg position. As the crystal setting approaches the Bragg position from either side, the scattering surface contracts and finally collapses at the reciprocal lattice point. This is illustrated by Fig. 14 which represents an example of slower-than-sound scattering surfaces, calculated by Lowde (1954), for different angular settings of an iron crystal. As the reciprocal lattice point is approached, fewer modes can contribute to the thermal diffuse scattering: however,

the contribution of each mode, proportional to q^{-2}, increases. Thus, to a rough approximation, the total cross-section for first-order scattering of slower-than-sound neutrons is substantially invariant with θ in the 2θ range near the Bragg reflexion, even though the scattering process changes over from phonon absorption to phonon emission at $\theta = \theta_B$. No TDS peak will occur at the Bragg position and so $\alpha = 0$. An exact calculation would require the mapping-out of the scattering surfaces (for the particular crystal under study) at different scattering angles 2θ, the integration of (2·13) over each surface to obtain the first-order diffuse intensity as a function of θ, and finally an estimate of the TDS correction, α, from the form of the diffuse intensity versus θ curve.

We conclude from this section that the first-order TDS correction for the scattering of faster-than-sound neutrons can be estimated from the same formulae as for X-rays, and that, to a first approximation, there is no correction for the scattering of slower-than-sound neutrons.

9. TDS correction of measured intensities

In § 6 we discussed some X-ray measurements on KCl and some recent neutron measurements on BaF_2. Both these sets of measurements were corrected for the effect of TDS, using the Cooper–Rouse treatment outlined in § 7·3, before being analysed in § 6 by the anharmonic theory. In this section, we shall describe the magnitudes of these TDS corrections and their influence on the isotropic B-factors of the constituent atoms.

9·1. Potassium chloride

James & Brindley's (1928) observations were made with an ionization chamber as detector, and to determine the general background scattering the measurements were repeated with the ionization chamber rotated by $2°$ from the Bragg position and the crystal off-set by $1°$. The intensities were recorded by means of an ω-scan. We shall assume that the oscillation angle of the crystal was $\pm 1·25°$ and that the detector had a square aperture subtending an angle of $1·5°$ at the crystal (see Nilsson, 1957).

The correction factor α, defined by equation (7·7), is listed in Table 6 for the six reflexions examined by James & Brindley at $20°C$. The second column gives the values of α derived by the Cooper–Rouse treatment: the TDS contribution to the measured intensity of the 400 reflexion is 3% of the zero-order (Bragg) intensity, whereas the proportion is as high as 24% for the 666 reflexion. The Nilsson treatment (see third column of Table 7) over-estimates the TDS correction, which is the expected consequence of assuming an infinite slit height for the detector. The difference between the α values for the finite and infinite slit heights is appreciable, and it is obviously desirable to use the correct slit height, as in the Cooper–Rouse treatment. The

fourth column of the Table gives the α's calculated from the spherical approximation, equation (7·9a), assuming $\Delta B = 0·18$ Å².

Table 6. TDS correction: KCl at $20°C$ (X-rays, Mo $K\alpha$)

$h_1 h_2 h_3$	α (Cooper–Rouse)	α (Nilsson)	α (spherical approximation)
400	3·3%	3·7%	3·6%
600	7·9	9·7	8·1
444	10·9	12·9	10·8
800	14·7	17·9	14·4
10,0,0	22·7	28·2	22·6
666	24·4	29·8	24·4

This choice of the artificial decrease ΔB in the overall temperature factor was made to give closest agreement with the estimates of α derived by the Cooper–Rouse procedure. Thus a very good TDS correction is possible using the spherical approximation, provided ΔB is known or is treated as an adjustable parameter.

9·2. Barium fluoride

Bragg reflexions were examined by Cooper, Rouse & Willis (1968) with slow neutrons of $\lambda = 1·037$ Å. This
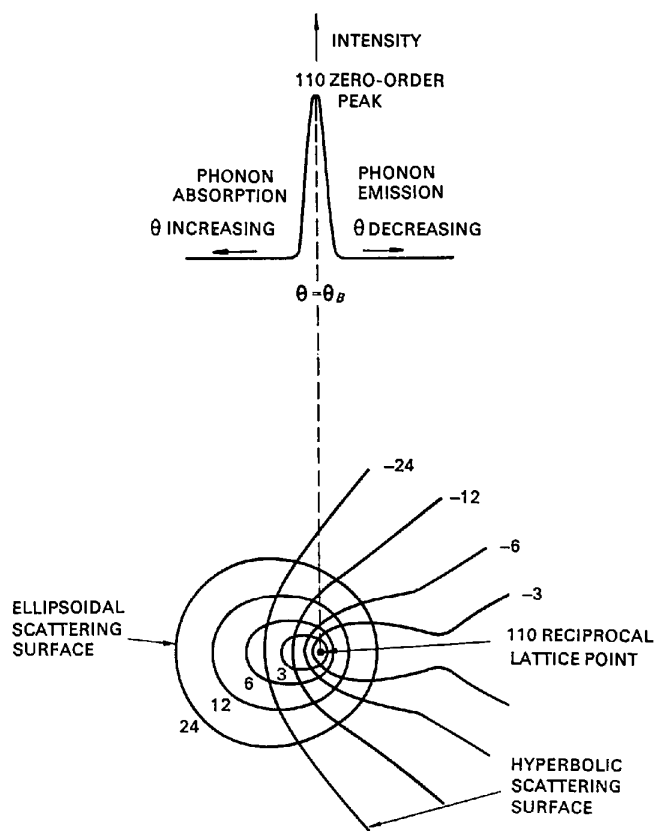

Fig. 14. Lower diagram: sections through the scattering surfaces for the first-order scattering of slower-than-sound neutrons by iron. The angles are marked in degrees relative to the Bragg setting (after Lowde, 1954). The upper diagram shows the scattered intensity versus θ.

wavelength corresponds to a neutron velocity of $3 \cdot 7 \cdot 10^5$ cm.sec^{-1}: we must determine first whether this is faster or slower than the acoustic modes of vibration in BaF_2.

At 20°C the elastic constants of BaF_2 (Gerlich, 1964) are:

$$c_{11} = 8 \cdot 92 \cdot 10^{11} \text{ dyne.cm}^{-2}$$
$$c_{12} = 4 \cdot 00 \cdot 10^{11} \text{ dyne.cm}^{-2}$$
$$c_{44} = 2 \cdot 54 \cdot 10^{11} \text{ dyne.cm}^{-2} .$$

The condition for elastic isotropy ($c_{11} - c_{12} = 2c_{44}$) is nearly satisfied, and so the velocity of the longitudinal acoustic wave is

$$|V_l| = \sqrt{c_{11}/\varrho} = 4 \cdot 3 \cdot 10^5 \text{ cm.sec}^{-1}$$

and the velocity of the two transverse acoustic waves is

$$|V_t| = \sqrt{c_{44}/\varrho} = 2 \cdot 3 \cdot 10^5 \text{ cm.sec}^{-1}$$

where the density $\varrho = 4 \cdot 9$ g.cm^{-3}. Thus the neutrons are slower than sound for the longitudinal modes and faster than sound for the transverse modes.

From the discussion in § 8, the TDS correction must be evaluated for the transverse modes only. Accordingly, the summation

$$\sum_{j=1}^{3} \frac{E_j(\mathbf{q}) \cos^2 \alpha_j(\mathbf{q})}{V_j^2}$$

in equation (8·2) is written ($E_j(\mathbf{q}) = k_B T$) as

$$\frac{k_B T}{2} \cdot \frac{2}{V_t^2}$$

whereas this would be expressed by

$$\frac{k_B T}{2} \left(\frac{2}{V_t^2} + \frac{1}{V_l^2} \right)$$

for the corresponding X-ray case.

The intensities were recorded by means of a $\theta/2\theta$-scan in which the crystal oscillated through $\pm 1 \cdot 2°$ and the BF_3 detector through twice this angle. The horizontal aperture of the detector was $\pm 1 \cdot 1°$ and the vertical aperture $\pm 1 \cdot 6°$. Table 7 gives the α-values for a few reflexions examined at 20°C, calculated both by the Cooper–Rouse treatment and by the spherical approximation with $\Delta B = 0 \cdot 05$ Å^2.

Table 7. TDS correction: BaF_2 at 20°C (1·04 Å neutrons)

$h_1 h_2 h_3$	α (Cooper–Rouse)	α (spherical approximation)
511	1·7%	1·8%
600	2·5	2·3
711	3·7	3·3
733	4·3	4·4
933	6·9	6·4
666	8·3	7·0

Agreement between the two sets of α is not as good as for Table 6 because the θ range is much larger in Table 7. The isotropic B-factors of the anion and cation in BaF_2 are appreciably different, but neglect of the TDS correction is roughly equivalent to an artificial reduction of each B-factor by 0·05 Å^2 at 20°C.

The results obtained in § 9 on KCl and BaF_2 can be summarized as follows:

(1) The TDS correction to the measured intensities can be very large – as much as 24% at room temperature for KCl – although not as large as the correction predicted by Nilsson (1957).

(2) The most satisfactory estimate of the TDS correction for cubic crystals is obtained from the Cooper–Rouse procedure, in which the dimensions of the detector aperture are taken into account properly. A further refinement of this procedure would include allowances for resolution effects (mosaic spread of crystal and divergence of incident beam) and for higher-order (multi-phonon) scattering. In both the Cooper–Rouse and Nilsson treatments, it is assumed that the mean value of $\cos^2 \alpha_j(\mathbf{q})$ in equation (7·2) is one third; this is true only for a spherical region surrounding the reciprocal lattice point, and in a more exact analysis the correction term α [equation (7·11)] would depend on the direction of $\mathbf{Q}$ as well as its magnitude. (For non-cubic crystals, it is essential to treat α as anisotropic in reciprocal space: see Rouse, Willis & Cooper, 1969.)

(3) Neglect of the TDS correction leads to an artificial lowering of the overall temperature factor. In selected cases, agreement (to about 1%) is still possible between observed and calculated intensities, provided that the individual atomic temperature factors are treated as adjustable parameters.

References

ANNAKA, S. (1962). J. Phys. Soc. Japan, 17, 846,

BUYERS, W. J. L. & SMITH, T. (1968). To be published.

CLARK, S. P. (1966). Handbook of Physical Constants, p. 80. New York: Geological Society of America.

COCHRAN, W. (1963). Reports Prog. Physics, 26, 1.

COOPER, M. J. (1969). In Electronic and Nuclear Density Distributions in Crystals. Oxford Univ. Press.

COOPER, M. J. & ROUSE, K. D. (1968). Acta Cryst. A24, 405.

COOPER, M. J., ROUSE, K. D. & WILLIS, B. T. M. (1968). Acta Cryst. A24, 484.

CRUICKSHANK, D. W. J. (1956). Acta Cryst. 9, 747.

DAWSON, B. (1967a). Proc. Roy. Soc. A298, 255.

DAWSON, B. (1967b). Proc. Roy. Soc. A298, 264.

DAWSON, B. (1967c). Proc. Roy. Soc. A298, 379.

DAWSON, B. (1967d). Proc. Roy. Soc. A298, 395.

DAWSON, B., HURLEY, A. C. & MASLEN, V. W. (1967). Proc. Roy. Soc. A298, 289.

DAWSON, B. & WILLIS, B. T. M. (1967). Proc. Roy. Soc. A298, 307.

EGELSTAFF, P. A. (1965). (Editor). *Thermal Neutron Scattering*. London: Academic Press.

GERLICH, D. (1964). *Phys. Rev.* **135**, A1331.

HAHN, H. & LUDWIG, W. (1961). *Z. Phys.* **161**, 404.

JAMES, R. W. (1962). *The Optical Principles of the Diffraction of X-rays*. London: Bell.

JAMES, R. W. & BRINDLEY, G. W. (1928). *Proc. Roy. Soc.* A**121**, 155.

KASHIWASE, Y. (1965). *J. Phys. Soc. Japan*, **20**, 320.

KRIVOGLAZ, M. A. & TEKHONOVA, E. A. (1961). *Soviet Physics Crystallography*, **6**, No. 4, 399.

LAGE, F. C. VON DER & BETHE, H. A. (1947). *Phys. Rev.* **71**, 612.

LONSDALE, K. (1962). In *Fifty Years of X-ray Diffraction*. Utrecht: Oosthoek.

LOWDE, R. D. (1954). *Proc. Roy. Soc.* A**221**, 206.

MARADUDIN, A. A. & FLINN, P. A. (1963). *Phys. Rev.* **129**, 2529.

NILSSON, N. (1957). *Ark. Fysik*, **12**, 247.

PASKIN, A. (1957). *Acta Cryst.* **10**, 667.

ROUSE, K. D., WILLIS, B. T. M. & PRYOR, A. W. (1968). *Acta Cryst.* B**24**, 117.

ROUSE, K. D., WILLIS, B. T. M. & COOPER, M. J. (1969). To be published.

SEEGER, R. J. & TELLER, E. (1942). *Phys. Rev.* **62**, 37.

SLATER, J. C. (1967). *Quantum Theory of Molecules and Solids*, Vol. 3. New York: McGraw-Hill.

SLATER, J. C. (1939). *Introduction to Chemical Physics*. New York: McGraw-Hill.

THOMPSON, B. V. (1963). *Phys. Rev.* **131**, 1420.

VALENTINE, T. M. & WILLIS, B. T. M. (1965). U.K.A.E.A. Report – R4939.

WILLIS, B. T. M. (1963*a*). *Proc. Roy. Soc.* A**274**, 122.

WILLIS, B. T. M. (1963*b*). *Proc. Roy. Soc.* A**274**, 134.

WILLIS, B. T. M. (1965). *Acta Cryst.* **18**, 75.

WILLIS, B. T. M. & TAYLOR, R. I. (1965). *Physics Letters*, **17**, 188.

ZIMAN, J. M. (1964). *Principles of the Theory of Solids*. Cambridge Univ. Press.

Apparent Doubling of Kikuchi Lines Inside Strong Bands

BY J. GJØNNES AND R. HØIER

Department of Physics, University of Oslo, Norway

AND D. WATANABE

Department of Physics, Tohoku University, Sendai, Japan

Doubling of Kikuchi lines inside strong bands has been reported previously in electron diffraction patterns from MgO. The 'doubling' is now explained as being due to two different lines, which at the particular wavelength employed in the experiment are very close. Owing to strong enhancement from multiple beam interactions inside the band, one of the lines is visible only in this region. Further examples of such doubling are shown in patterns from MgO and natural spinel. The observed patterns are compared with theoretical calculations.

In a recent paper on dynamic effects in diffuse scattering from MgO, doubling of the deficient (820) Kikuchi line inside the (002) band was reported by two of us (Gjønnes & Watanabe, 1966). A pattern showing the doublet is reproduced in Fig. 1. The doubling was not theoretically explained; it was pointed out, however, that 4-beam calculations revealed an appreciable enhancement of contrast inside the band for Kikuchi lines crossing the band at right angles. It is the purpose of this note to present an explanation of the reported 'doubling' as being due to two different lines, one of which is visible only inside the band because of enhancement from multiple beam interactions in this region.

This explanation occurred to us during further experimental and theoretical studies on Kikuchi lines from other crystals. Effects reminiscent of the doubling were occasionally observed, as in the pattern reproduced in Fig. 2, taken from a small chip of natural spinel, $MgAl_2O_4$. Inside the (400) band a double line is clearly seen. Detailed analysis of this pattern and comparison with a pattern taken at a different voltage revealed that this particular doublet was composed of the line (084) and the central part of the $(2n+1,\bar{9},\bar{5})$ envelope. On changing the voltage from 100 kV to 80 kV, the (084) line and the envelope were moved apart and there was no appearance of a doublet.

In view of this, we re-examined the MgO pattern (Fig. 1) and found that at wavelengths close to 0·044 Å (corresponding to 72·5 kV) there would be near overlap of the deficient lines (820) and (14,4,0). An independent determination of the wavelength using the Kikuchi lines $(\bar{2}0\bar{8})$, $(\bar{2}08)$ and (820), (see Fig. 1) gave $\lambda = 0\cdot04393 \pm 0\cdot00007$ Å assuming the value $a = 4\cdot2119$ Å (Brown, 1965) for the lattice constant of MgO. Assuming the weaker line in the doublet to be (14,4,0), we